

## ENVIRONMENTAL MONITORING OF BIO-RESTORATION ACTIVITIES USING GIS AND REMOTE SENSING



***Emil Bayramov***

2009  
Dept. of Physical Geography and Ecosystems Analys  
Centre for Geographical Information Systems  
Lund University  
Sölvegatan 12  
S-223 62 Lund  
Sweden





**ENVIRONMENTAL MONITORING OF BIO-RESTORATION  
ACTIVITIES USING GIS AND REMOTE SENSING**

**Emil Bayramov 2009**

**Master's Degree in Geographical Information Systems**

**Azerbaijan**

**Supervisor**

**Dr. Ulrik Mårtensson**

**Department of Physical Geography and Ecosystem Analysis**

**Lund University**

## ABSTRACT

The main goal of this research was the development of GIS and Remote Sensing based methodology for environmental monitoring of bio- restoration activities of disturbed vegetation cover along oil pipeline corridor.

For the achievement of the main goal, high – resolution multispectral IKONOS and FORMOSAT satellite images acquired during vegetation peak seasons in 2007 and 2008 were processed by polynomial triangulation and orthorectification. During this process using ground control points and digital elevation model, the positional accuracy of images was increased to 1m (RMSE).

Transects along pipeline route were collected and measured in terms of spatial location and vegetation cover percentage using quadrat based field estimation. Field estimated values for vegetation cover of transects were normalized to the acquisition date of satellite images.

Normalized Vegetation Difference Index (NDVI) was calculated from all satellite images acquired for 2007 and 2008. Normalization of areas affected by temporal factors was made for NDVI spatial grids calculated from FORMOSAT images to baseline IKONOS NDVI through a regression and further on they were mosaiced.

Correlation was done between 2007 and 2008 normalized vegetation cover for transects and mean NDVI values extracted from 2007 and 2008 satellite images for those transects. Based on the acquired equations, spatial grids of NDVI were recalculated to vegetation cover.

Based on the prepared spatial grids of vegetation cover along pipeline route, it was applied to geo-statistical calculations to determine vegetation cover re-growth trend.

Vegetation cover maps were developed along the pipeline route and also the map of vegetation cover re-growth between 2007 and 2008 were also produced.

This allowed determining areas with negative and positive vegetation cover re-growth and based on this to evaluate overall process of bio-restoration activities between 2007 and 2008 years.

**Keywords:** GIS, Remote sensing, Vegetation Cover, GPS, Photogrammetry, NDVI

## ACKNOWLEDGEMENTS

I would like to express deep gratitude to my parents for encouraging me in all my career and academic activities, for giving me the freedom to explore things on my own and trust to take the right decisions in my life, their selfless support during the years of my professional and academic development.

My special thanks to Prof. Ulrik Marterson for supervising my Master Thesis and also for developing of my level of GIS knowledge during LUMA-GIS program and many thanks to Prof. Petter Pilesjö for the organization of LUMA-GIS program on the high level.

I would like to express deep gratitude to Lund University – LUMA-GIS program and all Professors of this program for admitting me to this program and developing my level of knowledge in Geographical Information Systems and Remote Sensing.

My special thanks also go to Mr. Stefan Svenson (SWEDESURVEY & LANTMATERIET) who recommended me to this program and who involved me for working into the World Bank and SIDA projects for the development of Unified Land Registration and Cadastre Systems in Azerbaijan and other Former Soviet Union Countries.

I would like to express deep gratitude to my sister - biologist - Saida Aliyeva, Ph.D for her advice, critical comments and support over the whole process on creating this thesis and for prove reading, critical comments and putting this thesis into shape.

I would like to express deep gratitude to my local supervisor Dr. Prof. Chingiz Ismailov who supported me with advices on creating this thesis.

## CONTENTS

<b>1. INTRODUCTION.....</b>	<b>6</b>
<b>1.1. Goals.....</b>	<b>7</b>
<b>1.2. Study area.....</b>	<b>8</b>
<b>1.2.1. Baku-Tbilisi-Ceyhan Pipeline .....</b>	<b>8</b>
<b>1.2.2. Location and topography.....</b>	<b>9</b>
<b>1.2.3 Climate.....</b>	<b>11</b>
<b>1.2.4. Geology and Soil.....</b>	<b>11</b>
<b>1.2.5. Habitat.....</b>	<b>13</b>
<b>1.2.6. Hydrology.....</b>	<b>15</b>
<b>2. MATERIALS AND METHODS .....</b>	<b>16</b>
<b>2.1. Datasets.....</b>	<b>16</b>
<b>2.2. Pre-processing .....</b>	<b>18</b>
<b>2.2.1. Sequence of methodology stages .....</b>	<b>18</b>
<b>2.2.2 Collection of ground control points.....</b>	<b>19</b>
<b>2.2.3 Resolution Merge/Pan-sharpening.....</b>	<b>20</b>
<b>2.2.4. Polynominal triangulation.....</b>	<b>20</b>
<b>2.2.5 Orthorectification.....</b>	<b>23</b>
<b>2.3. NDVI to Vegetation Cover Recalculation.....</b>	<b>24</b>
<b>2.3.1. Calculation of NDVI.....</b>	<b>24</b>
<b>2.3.2 Collection of Transects.....</b>	<b>24</b>
<b>2.3.3 Normalization of FORMOSAT to IKONOS NDVI spatial grids .....</b>	<b>27</b>
<b>2.3.4 Regression analysis between Transects measured VC and NDVI.....</b>	<b>28</b>
<b>2.3.5 Recalculation of NDVI Spatial Grids to Vegetation Cover Grids.....</b>	<b>28</b>
<b>2.4. Geo-statistical Analysis and Mapping.....</b>	<b>28</b>
<b>2.4.1. Vegetation Cover Trends Geo-statistical analysis.....</b>	<b>28</b>
<b>2.4.2. Development of Vegetation Cover and Vegetation Cover Re-growth Maps .....</b>	<b>30</b>
<b>3. RESULTS .....</b>	<b>31</b>
<b>3.1. Collected Ground Control Points.....</b>	<b>31</b>
<b>3.2. Satellite images with increased resolution.....</b>	<b>31</b>

<b>3.3. Triangulated and orthorectified satellite images.....</b>	<b>32</b>
<b>3.4. Calculated and normalized NDVI Spatial Grids.....</b>	<b>34</b>
<b>3.5. Collected transects along pipeline corridor.....</b>	<b>37</b>
<b>3.6. Regression between transects' vegetation cover and NDVI.....</b>	<b>39</b>
<b>3.7. Vegetation Cover Spatial Grids.....</b>	<b>41</b>
<b>3.8. Geostatistical analysis results of vegetation cover grids.....</b>	<b>43</b>
<b>3.9. Spatial grid of NDVI gain coefficients.....</b>	<b>44</b>
<b>3.10. Re-growth status of On RoW Vegetation cover relative to Off RoW.....</b>	<b>45</b>
<b>DISCUSSION.....</b>	<b>48</b>
<b>4.1 Photogrammetric processing of satellite images.....</b>	<b>48</b>
<b>4.2 GIS and Remote Sensing processing.....</b>	<b>48</b>
<b>4.3 GIS and Remote Sensing in bio-restoration activities and practicality of achieved results for oil and gas field.....</b>	<b>49</b>
<b>4.4 Critical Issues of the developed methodology and recommendations.....</b>	<b>50</b>
<b>CONCLUSION .....</b>	<b>53</b>
<b>REFERENCES .....</b>	<b>54</b>
<b>APPENDIX 1, Table of Transect's list with Vegetation Cover and mean NDVI .....</b>	<b>56</b>
<b>APPENDIX 2, Example of Rational Polynominal Coefficients for satellite image .....</b>	<b>58</b>
<b>APPENDIX 3, Triangulation results for IKONOS and FORMOSAT images...60</b>	

## DEFINITIONS

**BTC:** Baku-Tbilisi-Ceyhan oil export pipeline

**On RoW:** Area with 44 m buffer along pipeline with disturbed vegetation cover

**Off RoW:** Area outside of 44 m buffer along pipeline with non-disturbed vegetation cover

**IKONOS:** A high resolution satellite launched in September 1999 that is capable of providing high-resolution multispectral image with resolution of panchromatic – 1 m and multispectral – 4.

**FORMOSAT:** A high resolution satellite launched in May 2004 that is capable of providing high-resolution multispectral image with resolution of panchromatic – 2 m and multispectral – 8 m.

**NDVI:** Normalized Difference Vegetation Index, an index derived from satellite reflectance data that measures 'greenness' of vegetation, a proxy for chlorophyll levels in a plant.

**NIR:** Near infrared portion of the electromagnetic spectrum, for example, as recorded by the NIR sensor on QuickBird (0.77 $\mu$ m- 0.88 $\mu$ m).

**Orthorectified satellite imagery:** satellite imagery corrected from relief distortions

**Triangulation:** Establishment of the geometry for the sensor relative to objects on the Earth's surface.

**GCP:** Ground Control Points, specific pixel on image data for which the output coordinates are known

**Habitat Endpoint:** The percent vegetation cover of undisturbed habitat that serves as the end point (or target) of the trend towards complete restoration.

**Project Area:** The area disturbed as a result of construction of the project, including the On RoW

**Transect:** A line normally defined by a measuring tape that is laid out along the ground in the areas selected for sampling.

**Quadrates:** A square frame of varying dimensions comprising a rigid material that, when placed on the ground (normally along transect), defines the boundaries of the sampling unit.

**Erosion Class:** A seven class classification system used to characterize erosion, ranging from very slight to catastrophic

**VIS:** Visible portion of the electromagnetic spectrum (0.4 $\mu$ m – 0.7 $\mu$ m).

**(DEM):** Continuous raster layers in which data file values represent elevation.

**KP:** Kilometer points along BTC pipeline generated from the origin of pipeline at the Sangachal Terminal



## **INTRODUCTION**

The research is focused on environmental monitoring of bio-restoration activities of vegetation cover along recently constructed onshore underground BTC (Baku-Tbilisi-Ceyhan) oil export pipeline in Azerbaijan. The research will cover the part of pipeline corridor over the territory of Azerbaijan. Azerbaijan is rich with the natural resources of oil and gas and for the exploration and exploitation of these resources it is often applied to the industrial construction activities. For the export of oil and gas resources different pipelines were constructed. In the process of construction, vegetation cover along pipeline was disturbed by excavation and construction activities. Vegetation Cover should be restored (reinstated) to its pre-construction state and pipeline construction footprint should disappear in accordance with the Azerbaijan environmental commitment regulations.

The main goal of this research is to develop a GIS and Remote Sensing based methodology for environmental monitoring of bio- restoration of vegetation cover along pipeline corridor.

For this research it was applied to high resolution multi-spectral satellite images to monitor vegetation cover re-growth and trend along the pipeline corridor between 2007 and 2008. The results, achieved using Geographical Information System and Remote Sensing, are used to calculate re-growth status and trend with statistical and visual GIS representation and to determine where re-growth trend is positive or negative and where intervention by human is necessary. This methodology is supposed to be for non-agricultural areas since they are not impacted by anthropogenic activities.

First peculiarities of this research is that it deals with quite a detailed scale of territory and that's a reason why it was applied to high resolution and accuracy multi-spectral satellite images. The second peculiarity is that it can be applied as a practical collaborative environmental management system (Bayramov, et al, 2008). Moreover dealing with this detailed scale of territory it is necessary to consider remote sensing corrections to avoid of significant discrepancies in the final results.

## **1.1. Goals**

The general goal of this research is the development of methodology for environmental monitoring of bio-restoration for vegetation cover re-growth trend along oil pipeline corridor using GIS and Remote Sensing.

The detailed objectives are the following:

1. Correction of geometrical and positional accuracy for the IKONOS 2007 and FORMOSAT 2008 satellite images along pipeline by photogrammetric processing to accurately overlay them between each other and with the ground truth data (transects)
2. Development of NDVI from geometrically corrected satellite images of 2007 and 2008, normalization of FORMOSAT 2008 NDVI spatial grids affected by temporal factors, normalization of NDVI 2007 and NDVI 2008 to Vegetation Cover using ground truth data
3. Development of vegetation cover and re-growth maps for 2007 and 2008 along pipeline corridor
4. Development of overall statistical assessment of vegetation cover distribution between 2007 and 2008, development of relative re-growth statistics between disturbed and non-disturbed areas along pipeline corridor
5. Overall monitoring and assessment of bio-restoration activities along pipeline and planning of bio-restoration activities for 2009

Questions to be answered:

What is the status of bio-restoration activities between 2007 and 2008 on the detailed level and in the overall statistical terms?

Which areas along pipeline corridor require a continuation of bio-restoration activities?

Does this way of environmental monitoring fit the requirements for the evaluation and planning of the bio-restoration activities?

Which practicality does the results of this research hold for the future activities along the pipeline corridor?

Which are the critical aspects of this methodology in the achievement of accurate results?

## 1.2. Study area

### 1.2.1. Baku-Tbilisi-Ceyhan Pipeline

BTC pipeline starts in Azerbaijan from Sangachal Terminal on the coast of the Caspian Sea and passes through Georgia and Turkey territory and it ends at Turkey Ceyhan Marine Terminal where from oil is exported through Mediterranean Sea (Figure 1.1). Total length of the pipeline passing through Azerbaijan is 442 km. Oil exploration is being conducted in the Caspian Sea and a total of 10 million barrels of oil from Azeri-Chirag-Gunashli oil fields in the Azerbaijani sector of the Caspian Sea was required to fill pipeline.

The buffer zone of 22 m to both sides of buried BTC pipeline (Figure 1.2) is named on Right of Way (On RoW) and areas outside of pipeline 44 m corridor (On RoW) is named off Right of Way (Off RoW). Vegetation cover was disturbed along On RoW and bio-restoration activities like seeding and sawing are being implemented inside On RoW.

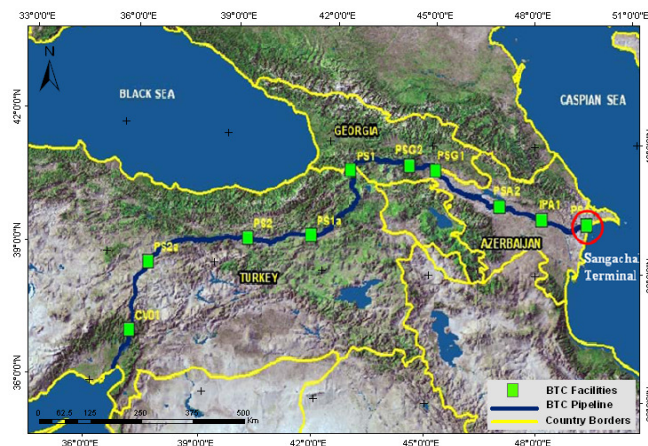


Figure1.1: Map of BTC pipeline over Azerbaijan, Georgia and Turkey.

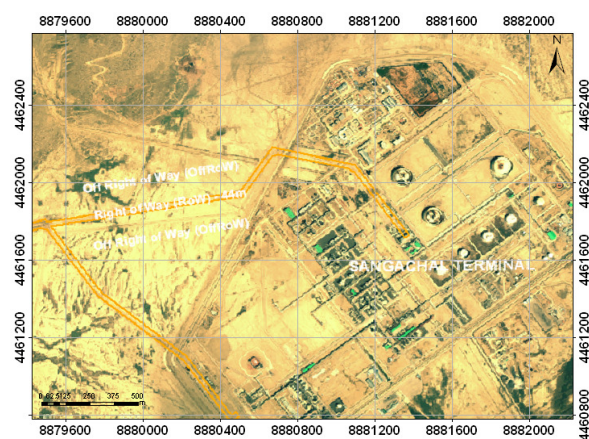


Figure1.2: On RoW and Off RoW of Sangachal terminal pipeline part.

### 1.2.2. Location and topography

Azerbaijan is predominantly a mountainous country. It is surrounded by three mountain ranges (AETC (Azerbaijan Environmental Technology Centre) LtD/ERM, 2002; Aliyev, F. et al, 2006). The Greater Caucasus form part of the northern border and include the nation's highest peak (4,466m) (Figure 1.4, 1.6). The Lesser Caucasus (Figure 1.4, 1.7) consists mostly of mountainous folds with peaks up to 3,900m orientated in a south-easterly direction. In the extreme south-east are the smaller but ecologically and geographically distinct Talysh Mountains (to 2,477m) (Figure 1.10). The remaining area of the territory consists of lowlands and plains, 18% of it below sea level. Chief among these is the central, flat, alluvial Kura-Araz and Upper Kura-Araz Lowlands (Figure 1.5, 1.8), through which the BTC pipeline in Azerbaijan is routed (Figure 1.5, 1.8). The Kura and Araz Rivers divide these lowlands into three parts: the Shirvan plain, north of the Kura River; Mil-Karabakh plain, between the Kura and the Araz Rivers (AETC LtD/ERM, 2002); and the Mugan plain, south of the Araz towards the lower reaches of the Kura River (Figure 1.3). From the eastern part of Azerbaijan is located the Caspian Sea and the coastal zone of it is characterized as the Coastal landscape (Figure 1.3, 1.9).

For understanding of geographic location it is necessary to refer to Figure 1.3 and 1.4. As supplementary information, kilometre points were added along the BTC pipeline to make it for easier visual observation.

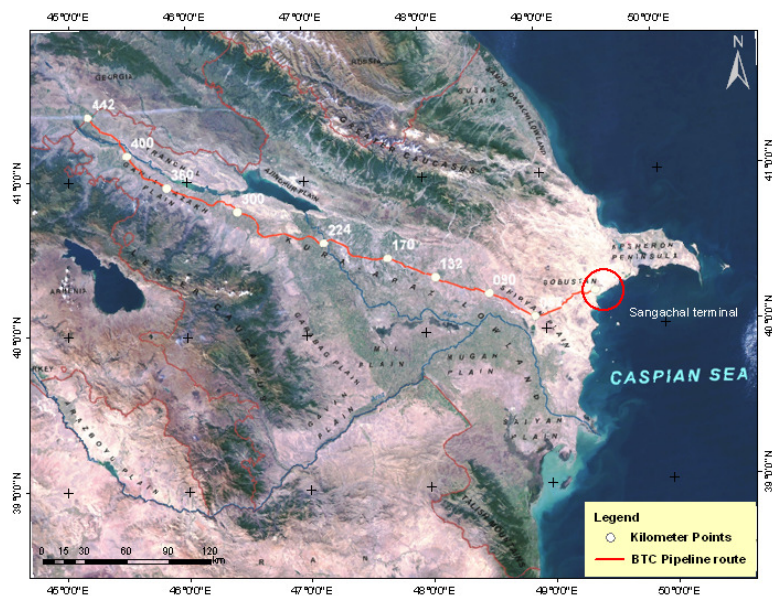
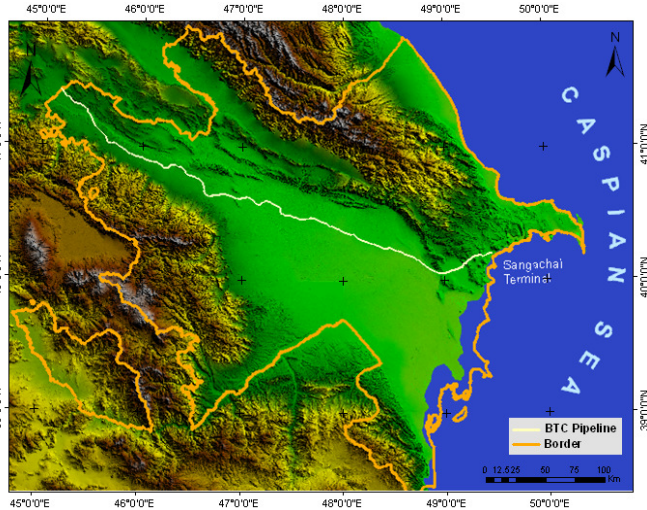
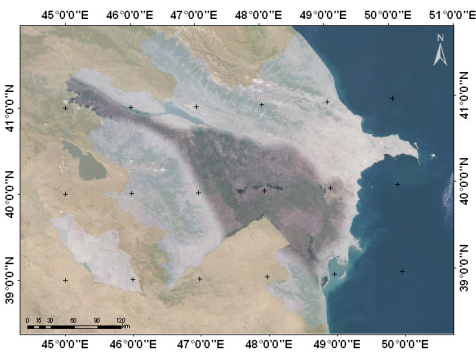


Figure 1.3: Location of BTC pipeline in Azerbaijan with kilometre points.



**Figure 1.4: Relief of Azerbaijan.**



**Figure 1.5: Kura-Araz Lowlands**

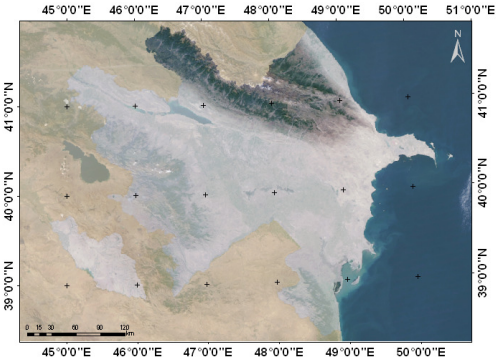


**Figure 1.6: Greater Caucasus Mountains**

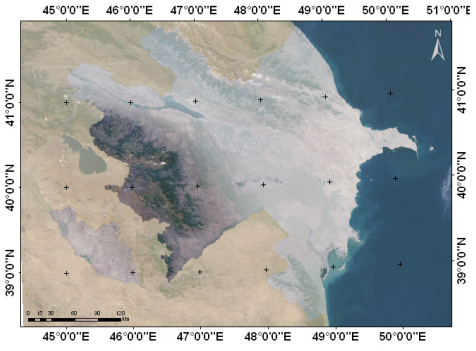


**Figure 1.7: Lesser Caucasus Mountains**

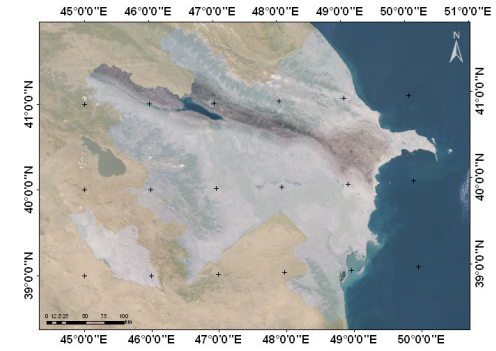


**Figure 1.8: Upper Kura – Araz Lowlands**

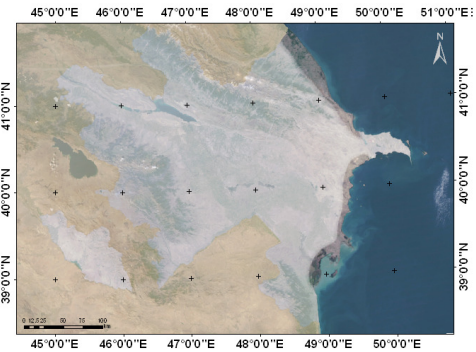


**Figure 1.9: Coastal Landscape**

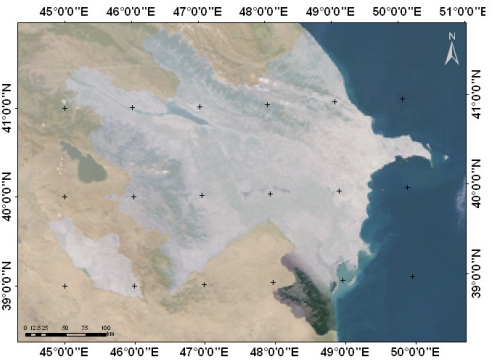


**Figure 1.10: Talysh Mountains**

### 1.2.3 Climate

Several climatic types can be differentiated in Azerbaijan, principally depending on the altitude of the area and distance from the Caspian Sea (AETC LtD/ERM, 2002; Aliyev, F. et al, 2006). The main climatic types are (Atlas of Azerbaijan Republic, 1979):

- Arid subtropical
- Humid subtropical
- Temperate
- Cold

The arid subtropical climate is typical for the Kura-Araz Lowlands where the main part of the BTC pipeline is located. The highest air temperatures occur in the Kura-Araz Lowland and along the Caspian Coastline (Bayramov, et al, 2006). Average July temperatures are more than +25°C; whilst during the winter temperatures rarely fall below freezing. The coldest month is usually January whilst the warmest months are July and August. It should be noted that much greater precipitation (and snowmelt) over the Caucasus ranges controls the magnitude and seasonal variation of flows in the rivers crossed by the pipeline (Figure 1.11).

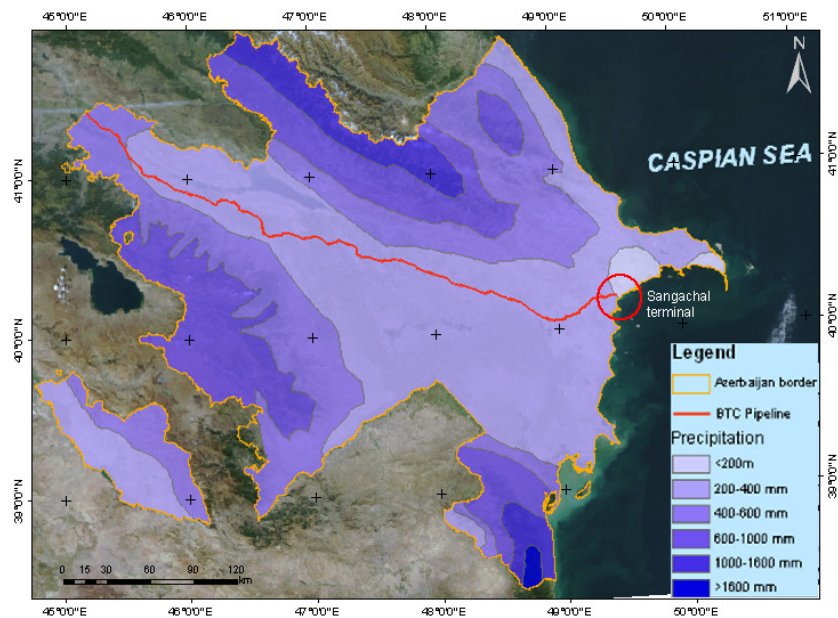


Figure 1.11: Precipitation map of Azerbaijan.

### 1.2.4. Geology and Soil

Cretaceous, Tertiary and Quaternary sedimentary rocks underlie the pipeline route in Azerbaijan (AETC LtD/ERM, 2002; Aliyev, F. et al, 2006). These rocks are

predominantly sandstones, lime stones and marls, with relatively minor sections underlain by metamorphic and igneous formations. Superficial quaternary cover of varying thickness and character mantles (underlying) rocks over most of the pipeline route. These deposits mainly consist of alluvial materials, although fluvial-glacial deposits and mud flows are also encountered. Mudflows from mud volcanoes occur only in the Gobustan region in the eastern part of the pipeline route (Figure 1.3, 1.9). The pipeline crosses a seismically active area where earthquakes of up to magnitude 8 on the Richter scale occurred. The highest densities of earthquakes occur north of the pipeline route in the foothills of the Great Caucasus, where strong earthquakes have led to the destruction of complete cities in the past (AETC Ltd/ERM, 2002). Soils in the eastern section (KP 0 to KP 52) generally consist of yellow brown silt and stony clays and loams with consistencies varying from soft and loose to slightly hard (Figure 1.12). Soil types in the legend of Figure 1.12 are based on the Atlas of Azerbaijan Republic produced in 1979.

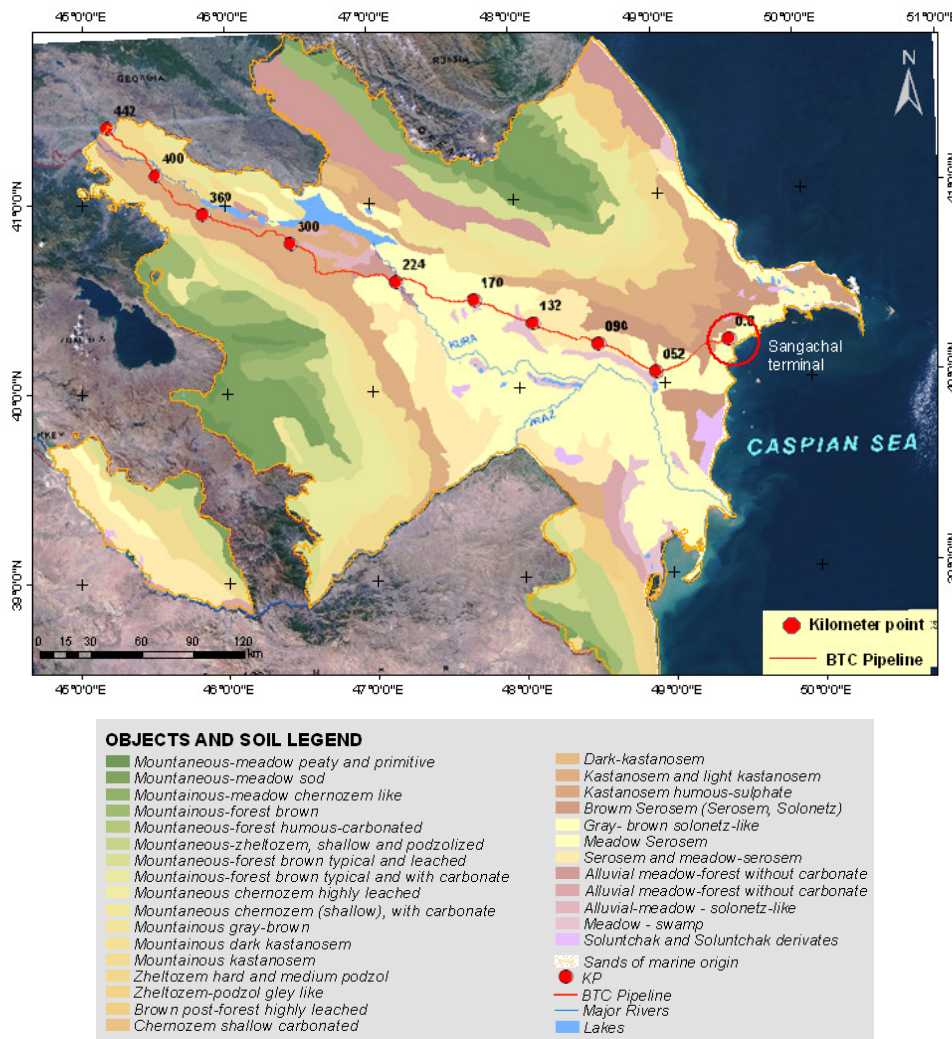


Figure 1.12: Soil map of Azerbaijan.

The soil structure is generally fine to medium. The soil surface often has a platy structure 3mm to 5mm thick that serves as a partial barrier to infiltration and contributes to high soil acidity. The topsoil in the Gobustan desert region, in particular, is very thin and has an elevated salinity, supporting sparse, saline tolerant vegetation.

Soils in the Central Region (KP 52 to KP 224) are depositional soils that are generally pale coloured (light yellowish brown) loams with a composition including significant quantities of silt, clay or sand. To the west (KP 128), the soil characteristics undergo a marked change (Figure 1.12). Unless currently irrigated, the surface tends to be highly cracked, with high concentrations of salt deposits seen on the surface. Poor irrigation practice in the past has been the principal contributor to soil salinity.

Western section soils (KP 224 – KP 442) include alluvial deposits between the two crossings of the Kura River (Figure 1.12). These deposits are typified by grey-brown silt, sandy and clayey loams, with high gravel and cobble content. Vegetation encountered is mixed, varying from natural uncultivated regions to semi-natural and agricultural lands (generally flat areas and valley floors). Erosion and deposition play major roles in soil formation in certain hill slope regions, so that in some regions gravel from inland areas covers soils lower on the slopes. The soils developed in this manner have little resistance to erosion, and when severely eroded lead to landscapes classified as badlands. At the western end of the route, from the Kura West River crossing (KP 411) to the Georgian border (KP 442), the soil is generally a light brown sandy or clayey loam (Figure 1.12). In the more easterly part of this section, the soils often consist of wet and waterlogged sands (AETC Ltd/ERM, 2002; Aliyev, F. et al, 2006).

### **1.2.5. Habitat**

The vegetation types along the pipeline have been categorized into 18 broad habitat types (Table 1.1). Habitat types along BTC pipeline on the Table 1.1 are based on the Vegetation of Azerbaijan map (1:1.000.000) prepared by L.I. PRILIPKO in 1970. Zoning of habitats along pipeline is developed based on the GPS measurements along pipeline corridor and the length for each habitat section in meters and in percentage (Table 1.1) was calculated based on the GIS spatial data of habitat zoning.



**Table 1.1: Habitats along BTC pipeline**

Habitat Type	Length, m	Length, %
Agricultural	305031.5	69.01165158
Alhagietum pseudoalhagi (Wetlands)	607.61	0.137468326
Artemisetum botriochloasum semi-desert (Semi-desert)	10965.57	2.48089819
Artemisetum lerchiana clayey desert (Desert)	36865.99	8.340721719
Artemisetum lerchiana purum desert (Desert)	7255.1	1.641425339
Capparisetum spinosa clayey desert (Desert)	1696.2	0.383755656
Chal meadow (Wetlands)	9012.97	2.039133484
Ephemeral desert (Desert)	6900.45	1.561187783
Fraxinetum woodland (Scrub and trees)	503.25	0.113857466
Halocnemetum strobilaceum solonchak desert (Desert)	16607.34	3.757316742
Phragmiteta - typhetum marsh (Wetlands)	410.34	0.092837104
Plantation Woodland (Scrub and trees)	838.55	0.189717195
Salsoletum dendroides clayey desert (Desert)	8893.02	2.011995475
Salsoletum nodulosae caleyey desert (Desert)	29426.19	6.65750905
Suaedetum microphylla solonchak desert (Desert)	1291.86	0.292276018
Tamarixetum scrub (Scrub and trees)	4804.52	1.086995475
Tugay forest (Scrub and trees)	540.55	0.12229638
Tugay forest (East) (Scrub and trees)	348.99	0.078957014
<b>Total</b>	<b>442000</b>	<b>100</b>

Generalised four types of habitats are represented on Figure 1.13 (a, b, c, d), taken along BTC pipeline.



**a. Desert and Semi – desert**



**b. Scrub and Trees**



**c. Agricultural Land**



**d. Forest**

**Figure 1.13: Pictures of habitats along BTC pipeline.**

### 1.2.6. Hydrology

The BTC pipeline route crosses 20 significant watercourses between KP 0 – 442. The route also crosses numerous streams, canals, drainage ditches and irrigation systems (Figure 1.14).

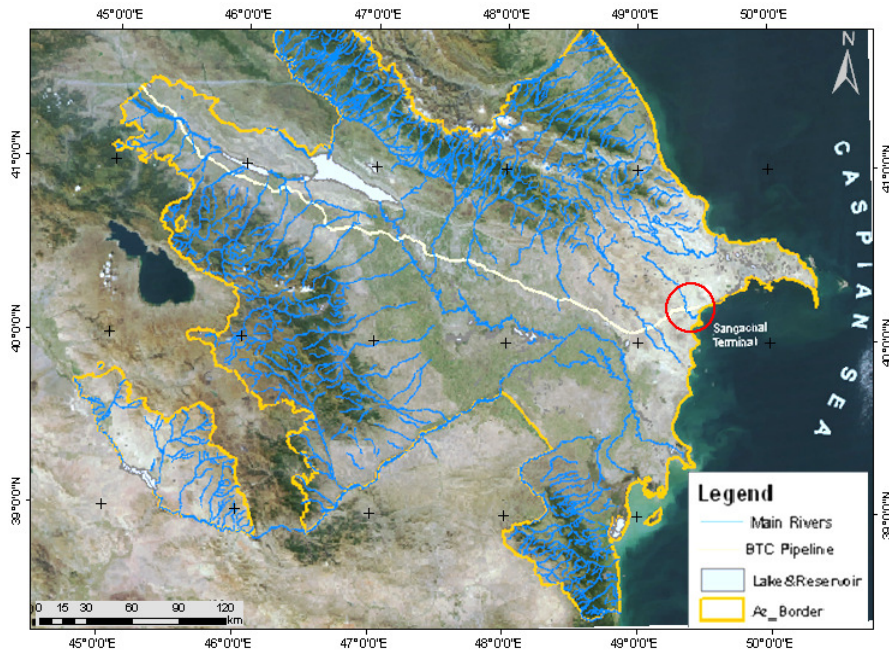


Figure 1.14: Hydrology map of Azerbaijan.

## **MATERIALS AND METHODS**

### **2.1. Datasets**

In order to achieve all results the following data were used:

- IKONOS - Satellite Imagery Acquired in 2007, Spatial resolution: Panchromatic: 1m, Multispectral (Blue, Green, Red, Near-infrared): 4m (Figure 2.1); Dates of images' acquisition: 04/18/2007, 05/01/2007, 06/04/2007, 07/23/2007, 07/24/2007 (Figure 2.1)
- FORMOSAT - Satellite Imagery Acquired in 2008, spatial resolution: Panchromatic: 2m, Multispectral (Blue, Green, Red, Near-infrared): 8m (Figure 2.2); Dates of images' acquisition: 05/07/2008, 05/16/2008, 05/17/2008, 05/20/2008, 05/22/2008, 05/23/2008, 05/29/2008, 06/02/2008, 06/11/2008, 06/13/2008, 06/14/2008 (Figure 2.2)
- Contour Lines and Digital Elevation Model - Generated from 1 m contour lines generated and edited from stereo aerial photography acquired in 2001;
- Field Collected Ground Control (GCP) points - GCP measured using high-precision GPS system with a positional accuracy of +/- 10 mm;
- Field Collected Transect data with evaluated vegetation cover for 2007 and 2008 – spatial location of transects measured by high-precision GPS with the accuracy of 50 cm and evaluated vegetation cover for them in 2007 and 2008.
- Calculated from satellite high-resolution multispectral images NDVI Spatial Grids for 2007 and 2008 - Normalized Difference Vegetation Index (NDVI) was calculated from geometrically corrected high – resolution multispectral satellite images;
- Pipeline Route and Pipeline Route corridor - Linear and polygonal object representing Baku-Tbilisi-Ceyhan pipeline route and 44m corridor buffer zone (Developed based on the high-precision GPS measurements)
- Habitat data - Habitat zones along Baku-Tbilisi-Ceyhan pipeline route with 250m buffer zone (Developed based on the GPS measurements along pipeline using habitat classification from the vegetation of Azerbaijan map prepared by L.I. PRILIPKO in 1970)
- Parcel and Land-use - Parcels along Baku-Tbilisi-Ceyhan pipeline route with 50 m buffer zone and land-use attributes (Developed based on high-precision GPS measurements along BTC pipeline)

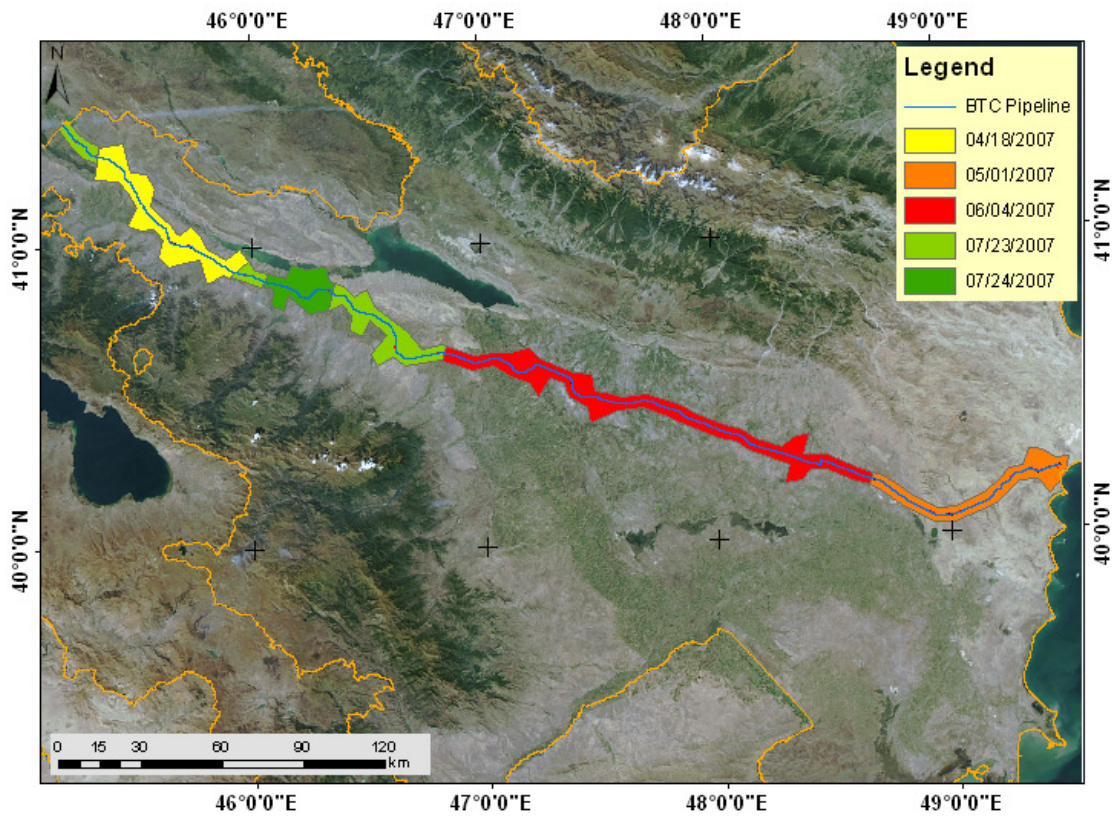


Figure 2.1: IKONOS satellite images acquired in 2007 along BTC pipeline.

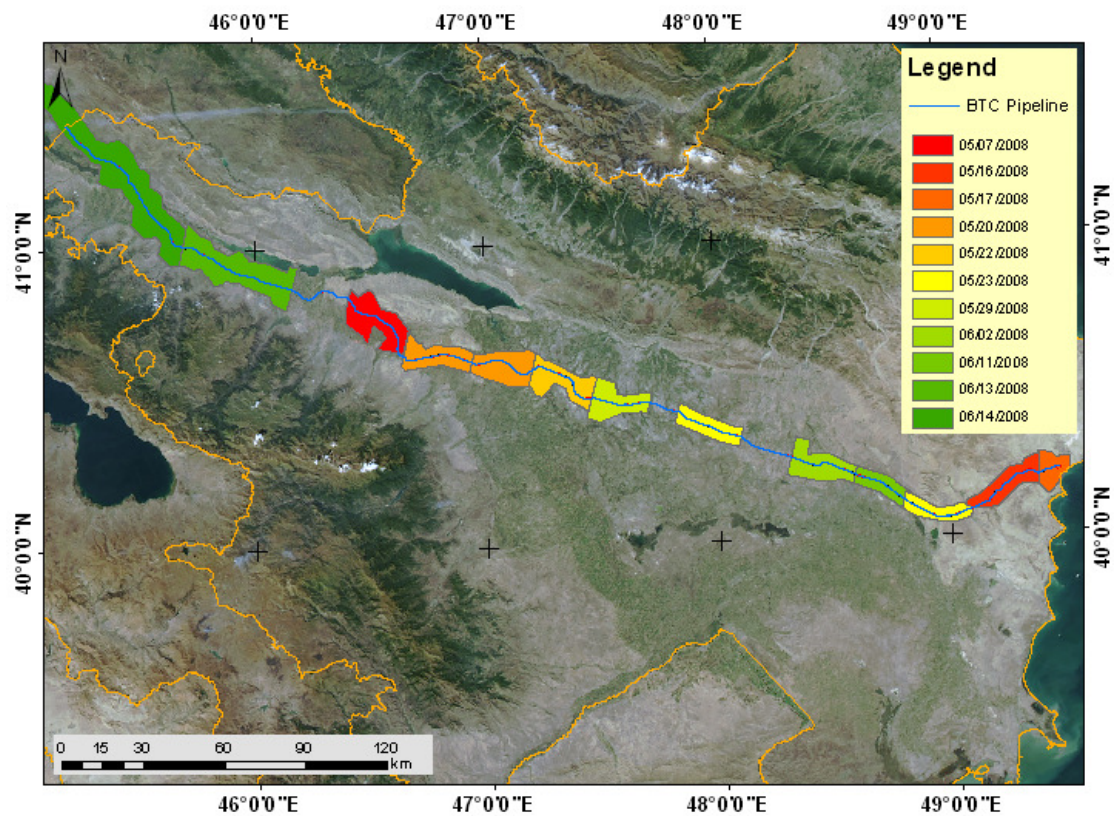


Figure 2.2: FORMOSAT satellite images acquired in 2008 along BTC pipeline.

## 2.2. Pre-processing

### 2.2.1. Sequence of methodology stages

The methodology stages of the complete process are presented on Figure 2.3. Three main applied basic methods are: photogrammetric processing to improve geometric and positional accuracy of satellite images, development of accurate vegetation cover using GIS and Remote Sensing and Geo-statistical analysis and mapping using GIS. Detailed description of methodology stages are presented in the further items in accordance with the sequence presented on Figure 2.3.

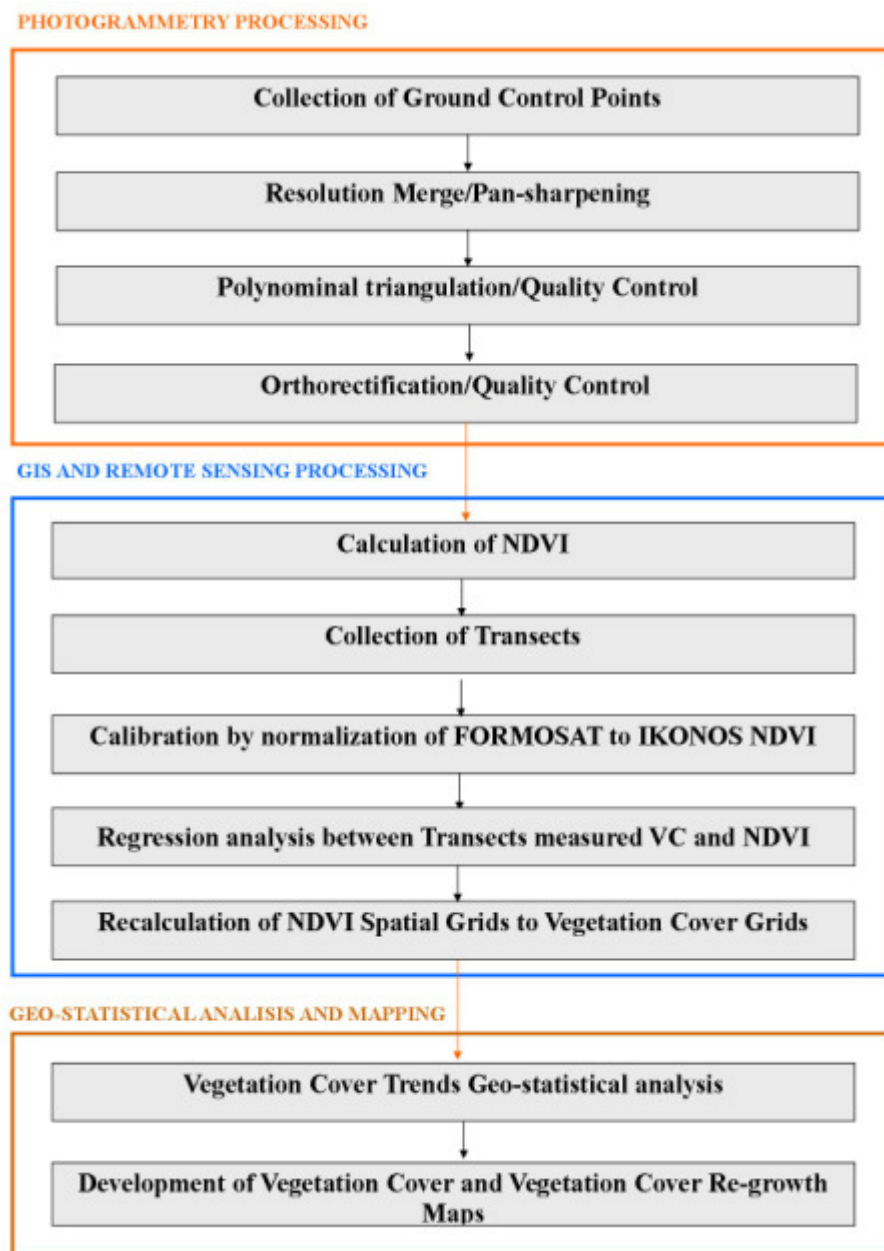


Figure 2.3: Complete sequence of methodology stages.

For the entire photogrammetric and remote sensing processing it was applied to ERDAS IMAGINE with Leica Photogrammetry Suite from Leica Geosystems and Socet Set from BAE Systems. For GIS spatial processing and analysis it was applied to ArcGIS (ArcInfo) 9.2 and its modules Spatial Analyst and 3D Analyst from Environmental Systems Research Institute (ESRI), ET Geowizard from ET Spatial Techniques and ArcPAD.

### 2.2.2. Collection of ground control points

Collection of ground control points was implemented using professional geodetic high-precision GPS equipment with dual-frequency and twenty-four channels. Measurement of Ground Control Points and Check Points was implemented in accordance with the following stages:

- Preliminary planning of optimum locations for Ground Control Points and Check Points based on raw satellite images and calculation of approximate x and y coordinates
- Identification of preliminarily planned Ground Control Points and Check Points in the field conditions;
- GPS-measurements of identified Ground Control Points and Check Points in the field conditions;
- Development of the Protocol Forms for the GPS measured Ground Control and Check Points (Figure 2.4).



GCP location on satellite imagery or field sketch	Photo for Measured GCP with positioned GPS
	
Identification Number of GCPs (or CPs)	
Brief description of location area	
Date/Measurement time	
Equipment/Serial Number No.	
Antenna Type	
Antenna height above ground level	
Survey Methodology Description	
GDOP	
Latitude, in decimal degrees, with 8 decimals after the point	
Longitude, in decimal degrees, with 8 decimals after the point	
Description of Quality Control Procedures	
Description of Statistical Analysis Procedures	
Standard Longitude Deviation	
Standard Latitude Deviation	
Standard Elevation Deviation	
Vertical datum	
Horizontal Datum	

Figure 2.4: Protocol form for GCP

### 2.2.3 Resolution Merge/Pan-sharpening

IKONOS and FORMOSAT satellite images are provided in the form of separate multispectral and panchromatic bands. IKONOS satellite image multispectral bands have spatial resolution of 4 m and panchromatic band of 1m. FORMOSAT satellite image multispectral band have spatial resolution of 8 m and panchromatic of 2m. By the process of resolution merge or also called a process of pan-sharpening it is possible to resample images of lower spatial resolution by higher spatial resolution images without changes in spectral characteristics (ERDAS Field Guide, 2005). This stage is preferable to be conducted since the research pipeline corridor has a width of 44 m and a resolution of images should be sufficient to achieve better visual results and by this process it is possible to raise IKONOS images resolution to 1 m and FORMOSAT images resolution to 2m (Figure 2.5). It is only being implemented to achieve higher visual quality of the final vegetation cover spatial grid product within 44 m corridor. Pan-sharpening process was done using resolution merging in the ERDAS IMAGINE software.

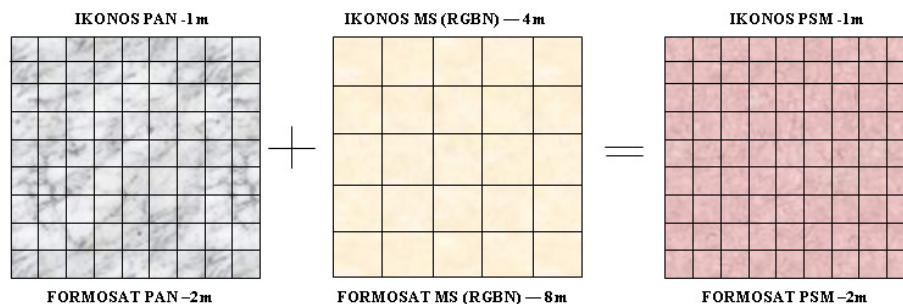


Figure 2.5: Resolution merge operation.

### 2.2.4. Polynominal triangulation

Geometric errors of satellite images are caused by the following variables, but are not limited to (ERDAS Field Guide, 2005):

1. Sensor orientation
2. Systematic error associated with the sensor
3. Topographic relief displacement
4. Earth curvature

Polynominal triangulation is applied to solve the errors caused by sensor orientation, systematic error associated with the sensor and earth curvature (ERDAS Field Guide, 2005).

In this research IKONOS and FORMOSAT imagery (Table 2.1) are supported by Rational Polynomial Coefficients (RPC) and these are coefficients of the relation between the image coordinates and the ground coordinates (Figure 2.6). There might be two types of provided supplementary information to satellite images - with rigorous sensor model or with rational function model (IKONOS Sensor Model Support Tour Guide, 2003). IKONOS images are always provided with rational functional model in the form of so called Rational Polynomial Coefficients (RPC) file (Amini, et al, 2005). But FORMOSAT imagery might be provided both with the Rigorous Sensor Model (RSM) and the Rational Function Model (RFM) supplementary information (Liu, et al, 2008). This supporting information is for determination of interior and exterior orientation, and it also contains supplementary information such as the geographic coordinates with defined projection that give preliminary geographic positioning of images (IKONOS Sensor Model Support Tour Guide, 2003). RPC data is accurate and it is possible to refine the accuracy of provided rational polynomial coefficients using Ground Control Points (Amini, et al, 2005, Bayramov, et al, 2004).

In the Rational Function Model, the image plane coordinates ( $r, c$ ) are expressed by ratio of two polynomials (Liu, et al, 2008; Liang-Chien, et. al, 2006) in which variables are relevant to ground coordinates ( $X, Y, Z$ ).

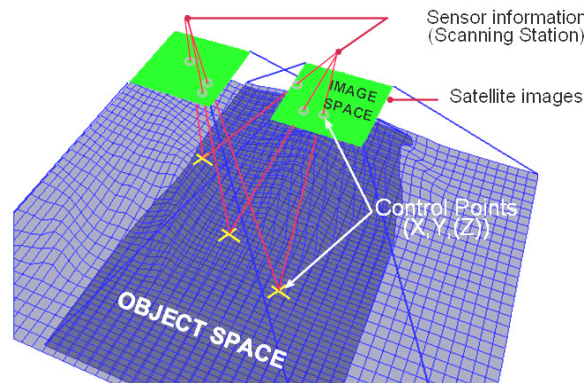


**Figure 2.6: Building relationship between sensor and ground**

Calculations are based on the following formulas (Liu, et al, 2008; Liang-Chien, et. al, 2006):

$$\begin{cases} r = \frac{p_1(X, Y, Z)}{p_2(X, Y, Z)} \\ c = \frac{p_3(X, Y, Z)}{p_4(X, Y, Z)} \end{cases} \quad (1)$$



where

(r, c) and (X, Y, Z) are normalized and dimensionless:

$$r = \frac{r_{raw} - r_{offset}}{r_{scale}}, c = \frac{c_{raw} - c_{offset}}{c_{scale}} \quad (2)$$

$$X = \frac{X_{raw} - X_{offset}}{X_{scale}}, Y = \frac{Y_{raw} - Y_{offset}}{Y_{scale}}, Z = \frac{Z_{raw} - Z_{offset}}{Z_{scale}}$$

The general form of polynomial  $P_i$  ( $i = 1, 2, 3, 4$ ) is:

$$P(X, Y, Z) = \sum_{i=0}^{n_1} \sum_{j=0}^{n_2} \sum_{k=0}^{n_3} c_{ijk} X^i Y^j Z^k \quad (3)$$

where:

$c_i$  is named as a Rational Polynomial Coefficient.

Depending on selected polynomial order of coefficient for correction, it is possible to correct different distortions in images caused by various factors (ERDAS Field Guide, 2005). Optical projection can be corrected by 1st-order polynomial coefficients. Earth curvature, atmospheric refraction and lens distortion can be corrected by 2<sup>nd</sup> - order polynomial coefficients and by 3<sup>rd</sup> - order of polynomial coefficients it is possible to make corrections to image against distortions caused by unknown factors. For the processing of images in this research it was applied to 3<sup>rd</sup> - orders of polynomials to reduce distortion maximally (Liu, et al, 2008; Liang-Chien, et. al, 2006). The accuracy that can be achieved during the triangulation is significantly dependent on the number of ground control points and their rational and overall distribution over satellite image areas (ERDAS Field Guide, 2005).

**Table 2.1: Satellite sensors' characteristics.**

<b>IKONOS SATELLITE SENSOR</b>	
Launch Date	September , 1999
Spectral Bands	Pan: 0.45 - 0.90 $\mu\text{m}$ ; Blue: 0.45 - 0.53 $\mu\text{m}$ ; Green: 0.52 - 0.61 $\mu\text{m}$ Red: 0.64 - 0.72 $\mu\text{m}$ ; Near-infrared: 0.77 - 0.88 $\mu\text{m}$
Spatial resolution	B&W: 1 meter, Multispectral (R, G, B, NIR): 4 meter
Swath Width	11 km x 11 km
Orbit Altitude	681 km
Orbit Inclination	98.1 degrees, sun-synchronous
Speed	7 km/second
Revisit Time	1.5-3 days depending on latitude
Image Dynamics	11 bits
Original Metric Accuracy (Horizontal)	12 m horizontal (RMSE)
<b>FORMOSAT SATELLITE SENSOR</b>	
Launch Date	May, 2004
Spectral Bands	Pan: 0.45 - 0.90 $\mu\text{m}$ ; Blue: 0.45 - 0.52 $\mu\text{m}$ ; Green: 0.52 - 0.60 $\mu\text{m}$ ; Red: 0.63 - 0.69 $\mu\text{m}$ ; Near-infrared: 0.76 - 0.90 $\mu\text{m}$

Spatial resolution	B&W: 2 meter , Multispectral (R, G, B, NIR): 8 meter
Swath Width	24km x 24km
Orbit Altitude	891 km
Orbit Inclination	99.1 degrees
Speed	7.2km per second
Revisit Time	Daily
Image Dynamics	8 bits
Original Metric Accuracy	50 m horizontal (RMSE)

Quality control of triangulation process using Ground Control and Check Points were also conducted based on the output triangulation reports which provided RMSE for each used points and total RMSE.

### 2.2.5 Orthorectification

Orthorectification process minimizes distortions appeared by impact of topographic relief displacement (Bayramov, E. R., 2007). The errors from topographic relief displacement can be corrected using Digital Elevation Model during the orthorectification procedure (Bayramov, E. R., 2007). Raw image with improved polynomial coefficients and Digital Elevation Model are applied for the process of orthorectification (Figure 2.7).

Relief displacement is corrected by taking each pixel of a DEM and finding the equivalent position in the satellite image. A brightness value is determined for this location based on resampling of the surrounding pixels (ERDAS Field Guide, 2005). The following parameters are important for the process of resampling the original image pixels into their new orthorectified positions: Pixel in the DEM (Figure 2.7, 1), Parameters of External Orientation (Figure 2.7, 2), Brightness determined based on the resampling of surrounding pixels (Figure 2.7, 3) and all together Height, Exterior orientation information and Brightness Value give possibility for calculation of equivalent location for the orthoimage (Figure 2.7).

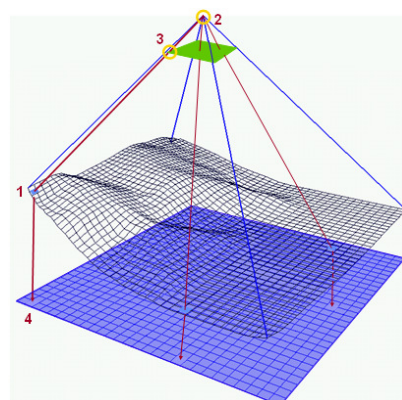


**Figure 2.7: Removal of relief distortions by DEM.**

**1-DEM; 2- External Orientation; 3-Image; 4- Ortho-image**

## 2.3. NDVI to Vegetation Cover Recalculation

### 2.3.1. Calculation of NDVI

NDVI (Normalized Difference Vegetation Index) is an index derived from satellite reflectance data that measures ‘greenness’ of vegetation, a proxy for chlorophyll levels in a plant (Bechtel, et al, 1997; Huete, et al, 1994, Leprieur, et al, 2000). The satellite data is processed to generate NDVI that essentially allows areas covered by vegetation to be distinguished from bare ground, and is derived from the following equation (ERDAS Field Guide, 2005):  $NDVI = (Band\ 4\ (Near\ Infra\ Red) - Band\ 3\ (Red)) / (Band\ 4\ (Near\ Infra\ Red) + Band\ 3\ (Red))$ , (Table 2.2).

**Table 2.2: Sequence of bands in IKONOS and FORMOSAT**

Imagery	IKONOS	FORMOSAT
Band 1	Blue	Blue
Band 2	Green	Green
Band 3	Red	Red
Band 4	Near Infra Red (NIR)	Near Infra Red (NIR)
Resolution after pan-sharpening	1 meter	2 m

NDVI is derived from satellite data recorded to coincide with peak chlorophyll levels, i.e., late Spring/early summer. Timing is necessarily vary with location and shall be based on field observations. To the extent possible, the collection of field data for ground truthing purposes should occur within the time planned for acquisition of images. Optimum timing of satellite data acquisition specific for Azerbaijan vegetation cover is April - July.

NDVI values should be determined for both On RoW (disturbed) and also for Off RoW (adjacent, undisturbed areas) for the purposes of assessing the ‘original’ vegetation cover.

### 2.3.2 Collection of Transects

NDVI is not an intrinsic physical quantity, although numerous studies spanning many years have shown a positive and generally linear relationship between NDVI and vegetation cover (Bechtel, et al, 1997; Huete, et al, 1994, Leprieur, et al, 2000). This observation forms the basis of the null hypothesis which is that NDVI is unrelated to vegetation cover (Leprieur, et al, 2000).

The strength of the observed relationship between NDVI and vegetation cover has been shown to be influenced by a variety of biophysical factors such as plant

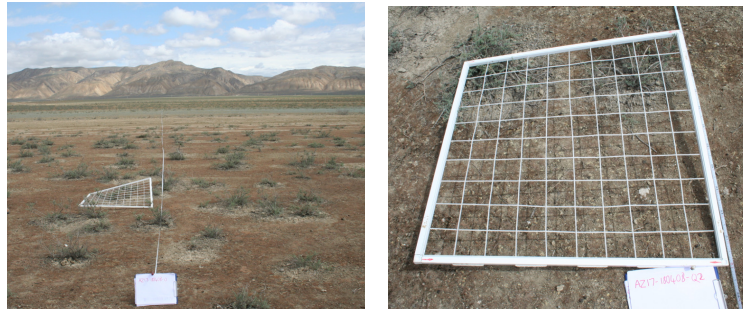
structure, background soil reflectance, shadow effects, solar and viewing angle, and atmospheric effects (Bechtel, et al, 1997; Huete, et al, 1994, Leprieur, et al, 2000). These factors vary locally, and hence there is a need to ground truth the satellite data, measure the strength of the correlation in different habitats, and use the information to determine re-growth trends.

Field measurement of vegetation cover involved the use of quadrat with the size of 1m x 1m and with a minimum sampling of 8 quadrates per transect where 5 is for On RoW and 3 is for Off RoW areas of transect. At each quadrat, vegetation cover was assessed by determining the relative proportion of bare ground to vegetation that can be seen when looking vertically onto the quadrat (Figure 2.9, 2.10). It is recorded as the percentage of vegetation to bare ground. Where interspatial gaps within a plant exist (i.e. space between branches within a plant) they were ignored. Thus, the edge of a plant serves as the cover boundary for an individual plant. Where plants are intersected by the frame of the quadrat, only that portion occurring inside the frame was considered as part of the percent cover estimate.

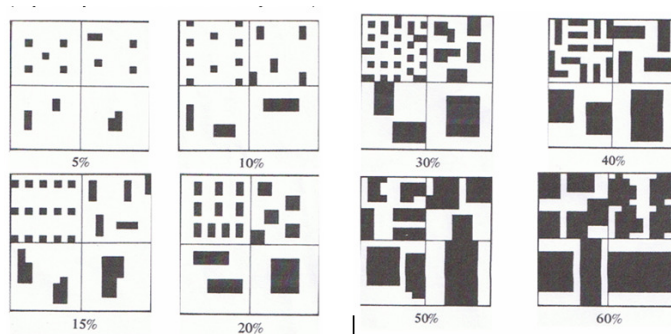
Percent vegetation cover was recorded in 10 percent intervals by visual evaluation of quadrates (0-10%, 11-20%, etc), using the median values of each interval (i.e., 5%, 15%, etc) to calculate an average percent cover for the On RoW portion of transect and a separate average for the Off RoW portion (Figure 2.9 and 2.10).



Figure 2.8: Transects along Off RoW and On RoW of BTC pipeline.



**Figure 2.9: Transects along BTC.**



**Figure 2.10: Measurement of vegetation cover by quadrat method.**

Since some transects and the percentage of vegetation cover for them were measured with difference in time to satellite images acquisition, it was necessary to normalize vegetation cover values in accordance with the generated theoretical re-growth curves (AETC LtD/ERM, 2002; Aliyev, F. et al, 2006) for each habitat both for On RoW and Off RoW (Figure 2.11). Based on the date of image acquisition, vegetation cover was interpolated from theoretical re-growth curves and the coefficient between theoretical and practically collected was calculated to normalize vegetation cover (Table 2.3) of field collected transects to dates of image acquisition.

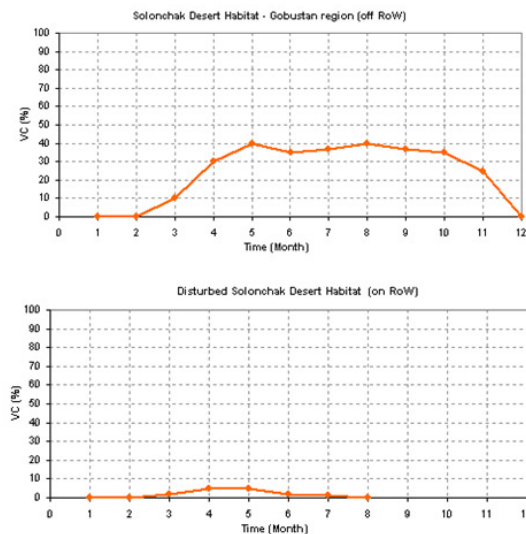


**Figure 2.11: Solonchak Desert habitat theoretical re-growth for On RoW and Off RoW.**

**Table 2.3: Number of Transects per habitat (2007-2008).**

Habitats along Pipeline Route	Number of Transects 2007-2008
Agricultural	0
Alhagietum pseudoalhagi (Wetlands)	0
Artemisetum botriochloasum semi-desert (Semi-desert)	5
Artemisetum lerchiana clayey desert (Desert)	3
Artemisetum lerchiana purum desert (Desert)	3
Capparisetum spinosa clayey desert (Desert)	3
Chal meadow (Wetlands)	4
Ephemeral desert (Desert)	3
Fraxinetum woodland (Scrub and trees)	0
Halocnemetum strobilaceum solonchak desert (Desert)	8
Phragmiteta - typhetum marsh (Wetlands)	1
Plantation Woodland (Scrub and trees)	4
Salsoletum dendroides clayey desert (Desert)	4
Salsoletum nodulosae clayey desert (Desert)	8
Suaedetum microphylla solonchak desert (Desert)	3
Tamarixetum scrub (Scrub and trees)	2
Tugay forest (Scrub and trees)	0
Tugay forest (East) (Scrub and trees)	2
Total	53

### 2.3.3 Normalization of FORMOSAT to IKONOS NDVI spatial grids

Normalization of NDVI values from different satellites images is sometimes necessary for some areas because NDVI values change for the same area because of difference in the spatial and spectral resolution of different satellite images and also other factors like atmospheric distortions etc. This difference may cause errors in analysis; therefore calibration should be made according to a baseline image. In this research, a baseline was selected IKONOS images since they have higher spatial and spectral resolution characteristics. In this research two FORMOSAT images – first and fifth images from the starting of pipeline corridor (Figure 2.2) were negatively affected by temporal factors and were providing reduced false NDVI values than it was in reality.. For the normalization of these FORMOSAT NVDI spatial grids to IKONOS, points were generated along Off RoW areas of pipeline corridor for the areas of these two images, because Off RoW was not disturbed during construction and vegetation cover did not significantly change naturally. Based on generated points, NDVI values were extracted to points from IKONOS 2007 and FORMOSAT 2008 NDVI spatial grids. Regression was applied to determine a correlation between IKONOS and FORMOSAT NDVI values extracted from these two images. Based on the acquired equations, FORMOSAT NDVI spatial grids of these two areas (Figure 3.8) were normalized to the baseline IKONOS NDVI range (Figure 2.12).

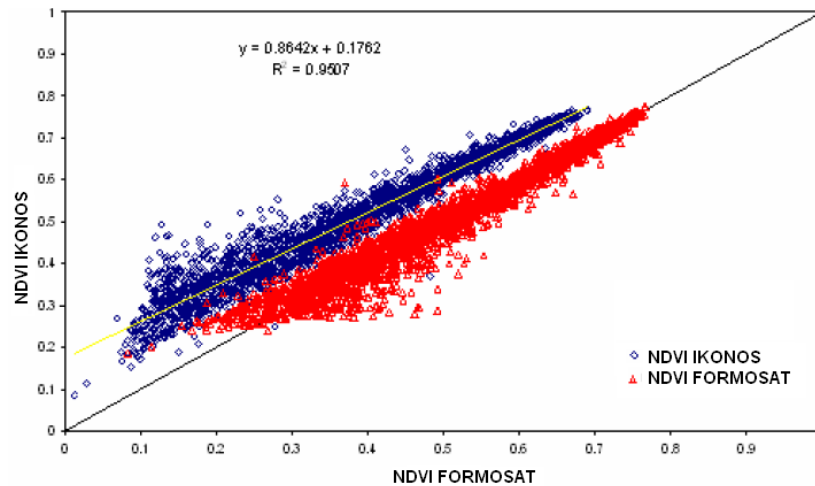


**Figure 2.12: Regression between IKONOS and FORMOSAT NDVI.**

### **2.3.4 Regression analysis between Transects measured VC and NDVI**

Regression analysis is for determination equivalent NDVI values for vegetation cover intervals (0-10%, 11-20%, etc). This allowed NDVI values to be calibrated against field measurements of vegetation cover, i.e, for a given NDVI value, a corresponding vegetation cover value was determined via the derived regression equation. The acquired equation from correlation between transects vegetation cover and NDVI was used for recalculation of NDVI grids to Vegetation Cover grids.

### **2.3.5 Recalculation of NDVI Spatial Grids to Vegetation Cover Grids**

After acquisition of equations for forest and non-forest habitats of 2007 and 2008, NDVI spatial grids for both 2007 and 2008 correspondingly can be recalculated to Vegetation Cover applying to raster calculator techniques for working with spatial grids.

## **2.4. Geo-statistical Analysis and Mapping**

### **2.4.1. Vegetation Cover Trends Geo-statistical analysis**

Based on the recalculated NDVI to vegetation cover spatial grids through the statistical ways, distribution of vegetation cover percentage per area was calculated and presented in graphs.

Afterwards entire On RoW corridor was divided into 100 m polygons and for each polygon mean NDVI value of both 2007 and 2008 was extracted from NDVI spatial grids. At the same time mean NVDI values were extracted for polygonal circles along

Off RoW of pipeline. The way of division of pipeline On RoW and Off RoW polygonal circles is presented on the Figure 2.13.

This was done to calculate overall re-growth trend of On RoW relative to Off RoW since Off RoW was not disturbed by human activities.

For the statistical overall representation of re-growth trend, based on the extracted mean values for each On RoW polygon and Off RoW polygonal circles from both sides of polygon, ratio between NDVI of On RoW and Off RoW (Formula 4) was calculated and to calculate regrowth trend of On RoW vegetation cover to Off Row it was necessary to extract Ratio 2007 from Ratio 2008 and divide it by absolute of Ratio 2007 (Formula 5).:

$$(\text{RoW NDVI}) / (\text{off RoW RefNDVI}) \quad (4)$$

$$\left( \frac{\text{Ratio 2008} - \text{Ratio 2007}}{\text{Abs (Ratio 2007)}} * 100 \right) \quad (5)$$



**Figure 2.13: 100 m On RoW polygons and 10m diameter Off RoW circular polygons.**

For the implementation of foregoing spatial grid overlay analysis it was necessary to apply to resampling of NDVI spatial grids to bring FORMOSAT extracted NDVI to the same resolution as extracted from IKONOS images that is 1 m (Figure 2.14).



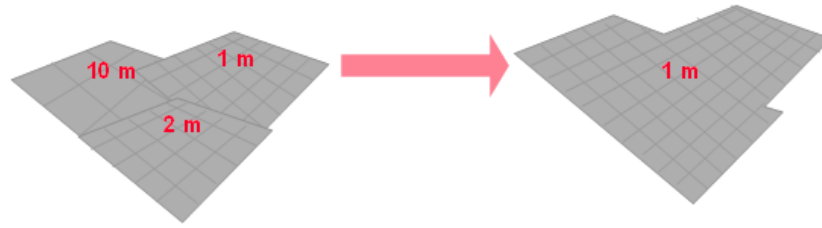


**Figure 2.14: Re-sampling to 1m resolution.**

Spatial grid of NDVI gain coefficients between 2007 and 2008 was calculated based on the subtraction of NDVI 2007 spatial grid from NDVI 2008 spatial grid. This was done using GIS overlay analysis of spatial grids applying to raster calculation techniques.

#### **2.4.2. Development of Vegetation Cover and Vegetation Cover Re-growth Maps**

This stage is dedicated to the development of maps which depicts vegetation cover at 10 % intervals and also to the development of maps for vegetation cover re-growth. Colour balancing (Hong, et al, 2007) was essentially applied to all satellite images to achieve good visual characteristics for using of them as backdrop images to vegetation cover and re-growth maps along BTC pipeline corridor.

## RESULTS

### 3.1. Collected Ground Control Points

As a result of stage for the collection of GCP, total number of collected of points is 218 points and they are rationally distributed over each satellite image along BTC pipeline route (Figure. 3.1). The accuracy for each of GPS measured points measured in RTK mode is +/- 10 mm. The collected points include both control and check points.

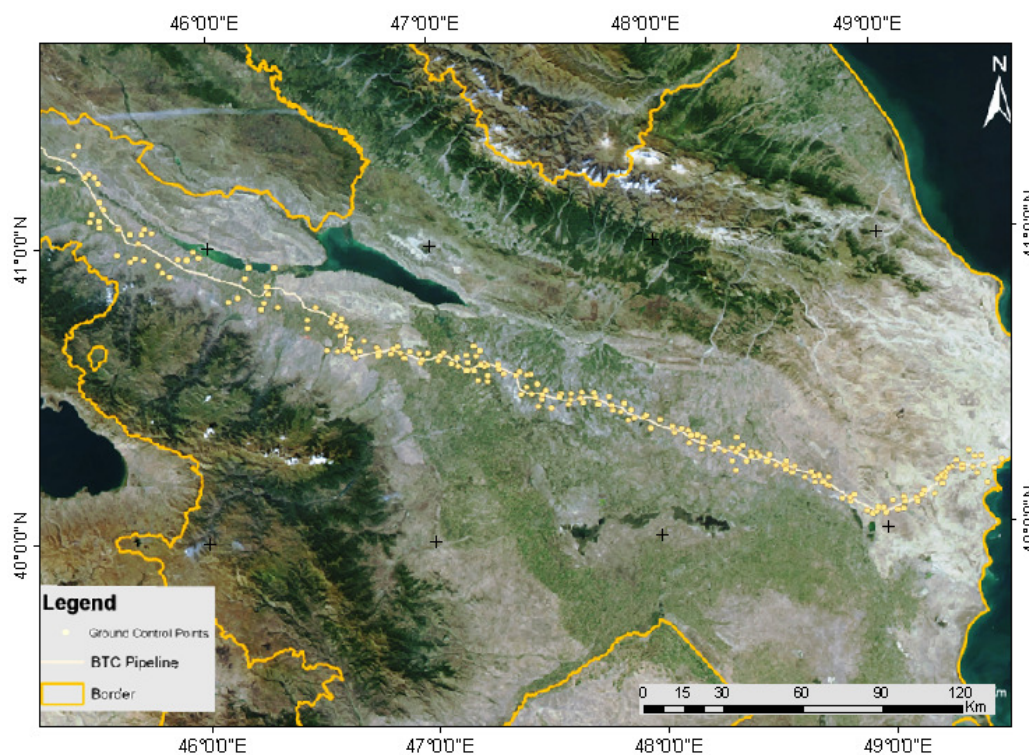


**Figure 3.1: Ground Control Points collected along BTC pipeline**

### 3.2. Satellite images with increased resolution

Pan-sharpening process stage allowed increasing the spatial resolution of IKONOS images to 1 meter and FORMOSAT images to 2 m without losing of spectral characteristics. This will only allow achieving better visual quality of the final vegetation cover spatial grids during the mapping process.

### 3.3. Triangulated and orthorectified satellite images

The stage of triangulation and orthorectification resulted in geometrically corrected satellite images - orthophotos along BTC pipeline route. All IKONOS 2007 and FORMOSAT 2008 images along BTC pipeline were triangulated and orthorectified. The resulted example of a triangulated and orthorectified image for area 1 on Figure 3.2 is presented. Total RMSE results of triangulation for the rest of IKONOS 2007 and FORMOSAT 2008 images are presented in Appendix 3.

RMSE achieved during polynomial triangulation for each image is up-to +/- 2 m. Triangulation and orthorectification results of the IKONOS 2007 and FORMOSAT 2008 images for the area 1 on Figure 3.2 along pipeline route are presented on (3.3, 3.5). Seven GCPs were applied for the triangulation and high – accuracy DEM (Figure 3.4, 3.6) acquired from aerial photography and presented in accordance with the triangulated satellite image area of interest (Figure 3.3, 3.5).

Since the accuracy of satellite images was improved to RMSE +/- 2m by photogrammetric processing it allowed to achieve high geometric and positional accuracy for overlaying of 2007 and 2008 satellite images between each other and also with transects, DEM, habitat, parcels and pipeline corridor.



Figure 3.2: Triangulated and orthorectified image of sample area 1 along BTC pipeline

Quality control of polynomial triangulation and orthorectification results of the IKONOS 2007 image for area 1 (Figure 3.2) is represented on Figure 3.3 and Table.3.1, 3.2.

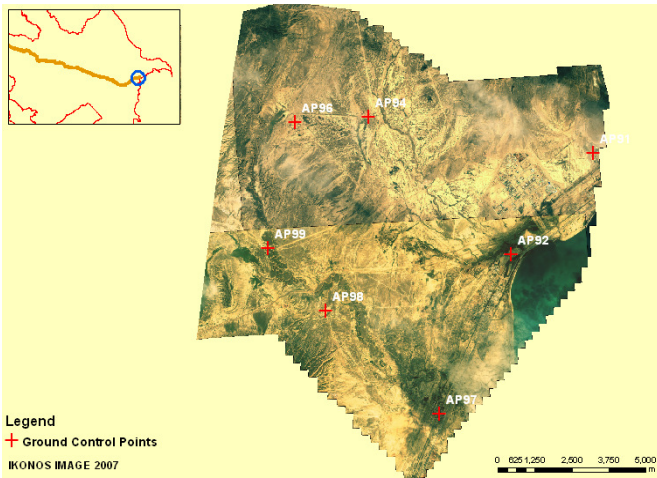


Figure 3.3: IKONOS image Triangulation for Area 1



Figure 3.4: DEM for Area 1

Table 3.1: RMSE of IKONOS Image for Area 1

Image of sample area 1	IKONOS							
	ID	Xin (WGS84)	Yin (WGS84)	Xref (WGS84)	Yref (WGS84)	XRes (px)	YRes (px)	RMSE (px)
	GCP 96	49.391533	40.224959	49.3912177	40.2236054	-0.2	0.57	0.6
	GCP 91	49.508807	40.2109429	49.50854	40.209602	0.04	-0.12	0.13
	GCP 92	49.474492	40.181565	49.4741413	40.1803228	1.49	0.5	1.57
	GCP 94	49.420943	40.2253969	49.4205297	40.2240731	-1.06	-0.15	1.07
	GCP 97	49.443038	40.1346352	49.4426901	40.1335807	-1.55	-0.29	1.57
	GCP 98	49.400174	40.1675005	49.3997549	40.166364	-0.83	0.18	0.85
	GCP 99	49.378336	40.187094	49.3781057	40.1858517	1.56	-0.48	1.63

Table 3.2: Total RMSE of IKONOS Image for Area 1

RMSE	PIXEL	METER
X	1.13	1.13
Y	0.37	0.37
TOT	1.19	1.19

Quality control of polynomial triangulation and orthorectification results of the FORMOSAT 2008 image for area 1 (Figure 3.2) is represented on Figure 3.5 and Table.3.3, 3.4.

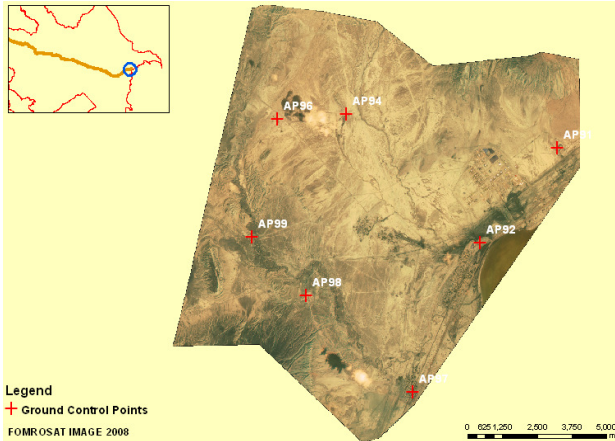


Figure 3.5: Formosat Sample Area 1 Triangulation.

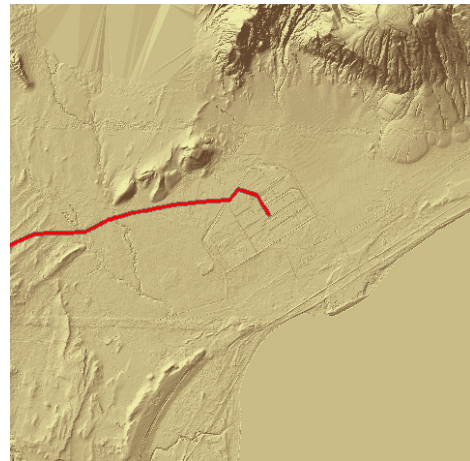


Figure 3.6: DEM for Sample Area 1.

Table 3.3: RMSE of FORMOSAT Image for Area 1

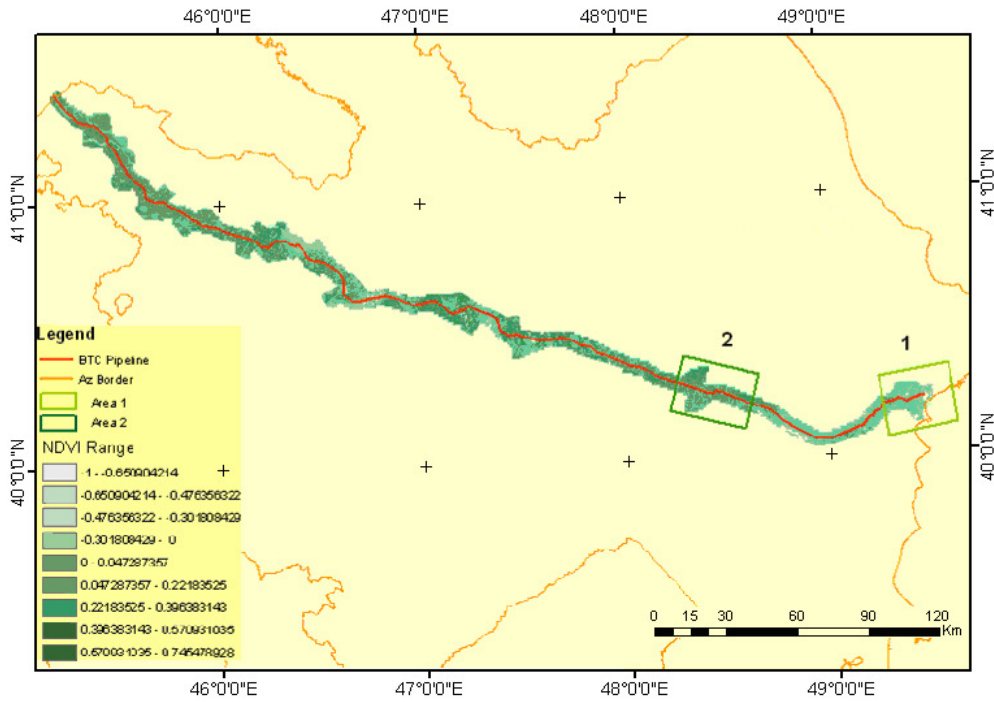
Image of sample area 1	FORMOSAT						
	ID	Xin (UTM WGS84)	Yin (UTM WGS84)	Xref (Gauss Kruger WGS84)	Yref (Gauss Kruger WGS84)	XRes (px)	YRes (px)
GCP 96	363075.06	4453821.4	8873922.13	4463707.36	0.0419	0.2557	0.2591
GCP 91	372980.9	4452090.86	8883992.23	4462653.86	0.3212	1.7729	1.8018
GCP 92	369999.51	4448888.63	8881226.61	4459252.45	-0.7689	-0.3919	0.863
GCP 94	365547.39	4453826.01	8876415.66	4463883.56	1.5111	-0.3644	1.5544
GCP 97	367265.7	4443754.39	8878806.83	4453924.81	0.3588	0.4062	0.542
GCP 98	363715.79	4447452.74	8874965	4457384.31	-0.8457	-0.396	0.9338
GCP 99	361875.83	4449649.23	8873012.91	4459457.88	-0.7164	-0.9419	1.1834

Table 3.4: Total RMSE of FORMOSAT Image for Area 1

RMSE	PIXEL	METER
X	0.79	1.58
Y	0.82	1.64
TOT	1.14	2.28

### 3.4. Calculated and normalized NDVI Spatial Grids

NDVI calculation resulted in NDVI spatial grids for each of IKONOS 2007 (Figure 3.7) and FORMOSAT 2008 images along pipeline corridor.



**Figure 3.7: NDVI Spatial Grids calculated from IKONOS images 2007.**

As a “Baseline NDVI”, it was applied to the calculated NDVI from IKONOS 2007 images (Figure 3.7) because of its high spatial and spectral characteristics (Table 2.1). Normalization of FORMOSAT NDVI spatial grids negatively affected by temporal factors for two areas (Figure 3.8) – first and fifth images from the starting of pipeline corridor (Figure 2.2) was made relatively to baseline IKONOS 2007 extracted NDVI spatial grids of areas 1 and 2 on Figure 3.7.

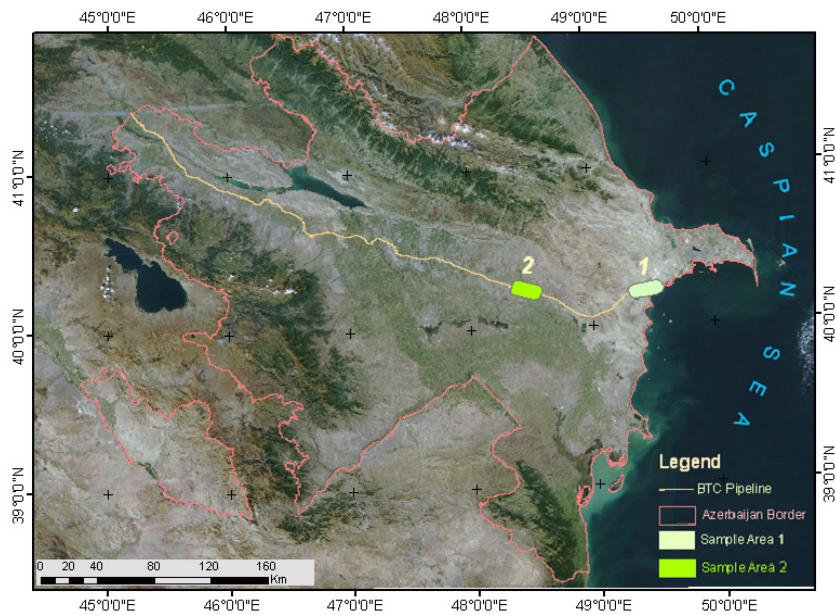


**Figure 3.8: Areas 1 and 2 affected by temporal factors and requiring normalization of FORMOSAT 2008 NDVI to IKONOS 2007 NDVI along BTC pipeline.**

The regression equations (Figure 3.9, 3.10) for two areas of interest (Figure 3.8) were achieved for the normalization of FORMOSAT 2008 NDVI spatial grids to IKONOS 2007 NDVI. Based on generated points (Figure 3.11, 3.12) along Off RoW (areas with non-disturbed vegetation cover) of pipeline corridor with extracted FORMOSAT 2008 and IKONOS 2007 NDVI values, the coefficients and equations of regression were acquired and were applied to normalize two areas (Figure 3.8) of FORMOSAT 2008 NDVI spatial grids to IKONOS 2007 using equations presented on Figure 3.9 for Area 1 and presented on Figure 3.10 for Area 2.

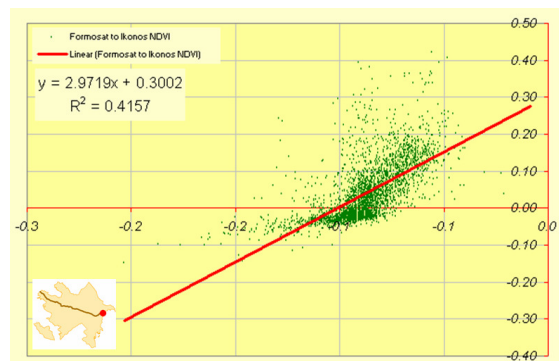


**Figure 3.9: Correlation of NDVI calculated from FORMOSAT 2008 and NDVI from IKONOS 2007 image for Sample Area 1.**

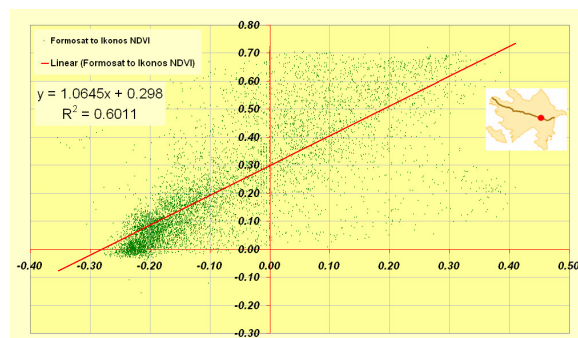


**Figure 3.10: Correlation of NDVI calculated from FORMOSAT 2008 and NDVI from IKONOS 2007 image for Sample Area 2.**

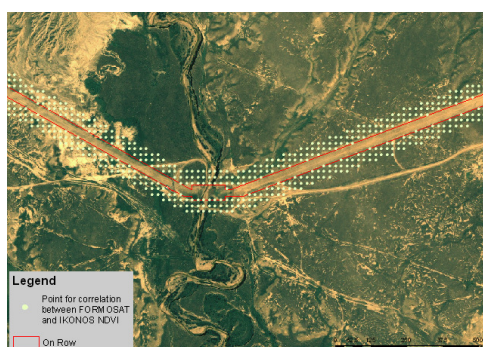


**Figure 3.11: Generated Points for Off RoW along BTC pipeline with extracted NDVI values from IKONOS NDVI spatial grid.**

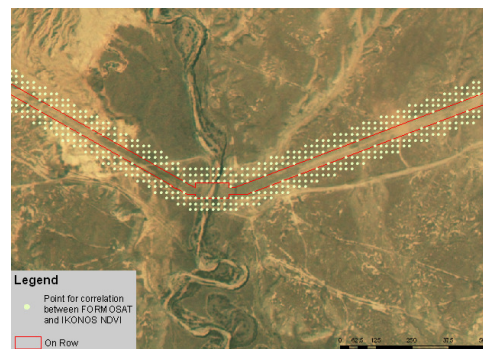


**Figure 3.12: Generated Points for Off RoW along BTC pipeline with extracted NDVI values from FORMOSAT NDVI spatial grid.**

As a final result of this stage for the calculation of NDVI from IKONOS images and calculation of NDVI from FORMOSAT images with normalization of two areas (Figure 3.8), NDVI spatial grids from IKONOS and FORMOSAT were mosaiced prioritizing spatial grids with higher NDVI in the overlapping areas along pipeline corridor and results were mosaiced IKONOS 2007 NDVI Spatial Grid and mosaiced FORMOSAT 2008 NDVI Spatial Grid for the entire pipeline route.

### 3.5. Collected transects along pipeline corridor

As a result of the stage for the collection of transects along BTC pipeline, it was measured 53 transects (Figure 3.13) where each transect consists of transect polygons (containing measured vegetation cover) for On RoW and Off RoW (Figure 2.8) and this means that total number of transect polygons is 106 for On RoW and adjacent Off RoW pipeline areas. Table of transects is represented in Appendix 1.

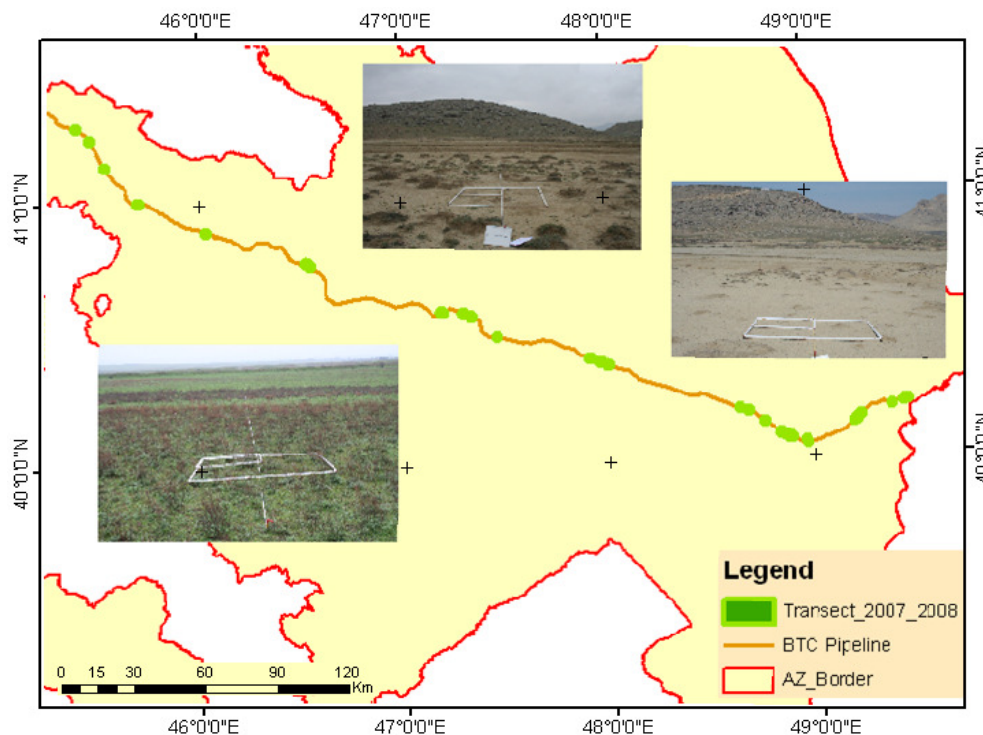


**Figure 3.13: Transects collected along BTC Pipeline.**

The results of transect monitoring without remote sensing analysis can be summarised as follows:

- There is an increasing trend in percentage of vegetation cover on most sections of the pipeline On RoW (Figure 3.14, 3.15)
- Few sections of the On RoW have a vegetation cover equal to that of adjacent, (Off



RoW) undisturbed vegetation (Figure 3.14)

- Some habitats are recovering more quickly than others.

The results also show that increase in vegetation cover is very slow in some habitats, particularly the arid and saline soils of the semi-desert habitats. These habitats are more common to the east of the pipeline, and Figure 3.14 shows that there is a general east-west trend of increasing vegetation cover. This is related to increasing suitability of habitats for establishment and survival of plants, related to soils and climate.

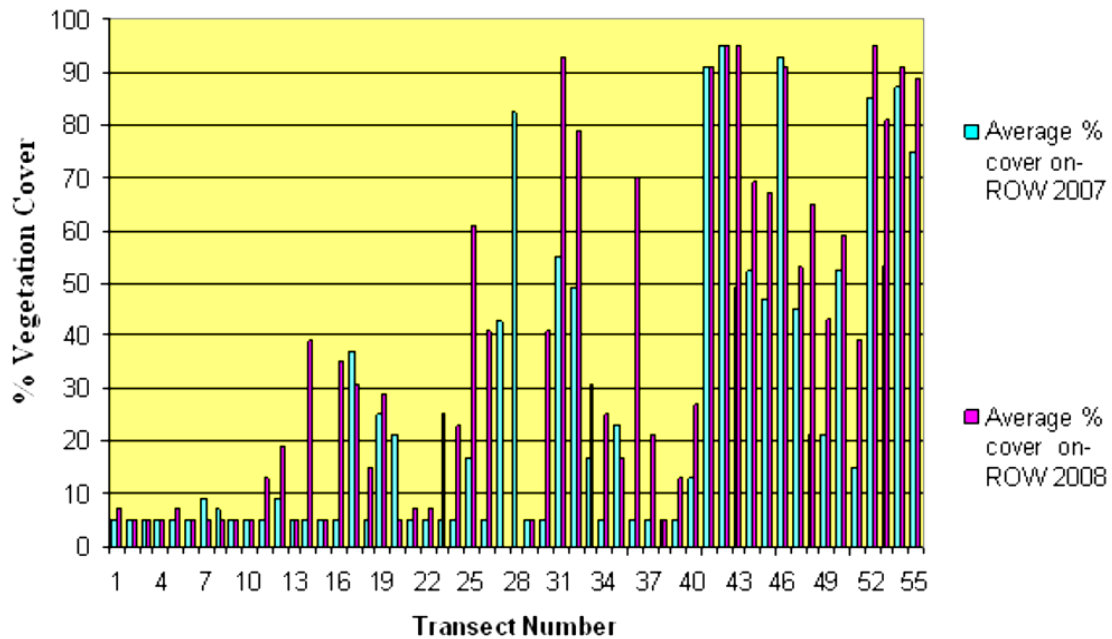


Figure 3.14: Vegetation Cover per transect polygon for On RoW between 2007 and 2008.

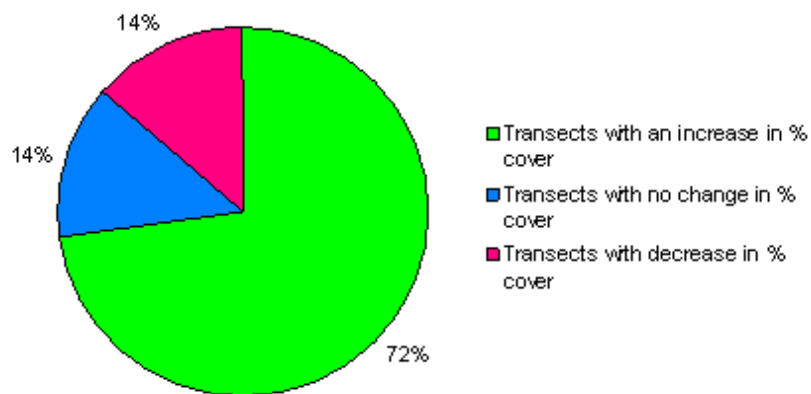
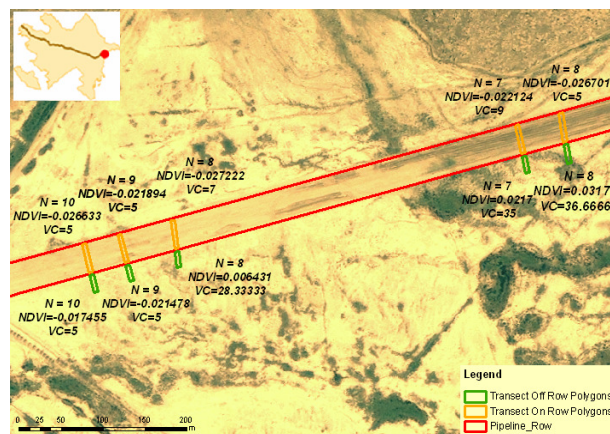


Figure 3.15: Proportion of transect polygons with an increase, decrease or no change in % vegetation cover between 2007 and 2008 for On RoW.

### 3.6. Regression between transects' vegetation cover and NDVI

As a result of regression analysis between extracted averaged IKONOS 2007 NDVI and FORMOSAT 2008 NDVI values for each transect polygon from NDVI spatial grids and vegetation cover percentage 2007 and 2008 collected by field measurements for the same transect polygons (Figure 3.16, 3.17), it was possible to achieve equations necessary for the recalculation stage of NDVI Spatial Grids to Vegetation Cover Spatial Grids. NDVI and Vegetation Cover Regression for the entire pipeline route (Figure 3.18, 3.19, 3.20, 3.21, 3.22, 3.23) was achieved separately for non-forest transects, forest transects and also for all transects. Number of transect polygons, applied during regression for each year, differed since some transects were negatively affecting to the overall results of regression because of two possible reasons as incorrectly evaluated vegetation cover or incorrectly extracted NDVI values, that's why in the process of regression some transects were excluded.



**Figure 3.16: Sample transects' polygons with extracted NDVI from IKONOS NDVI spatial grids and with field measured Vegetation Cover for 2007 (backdrop – IKONOS).**

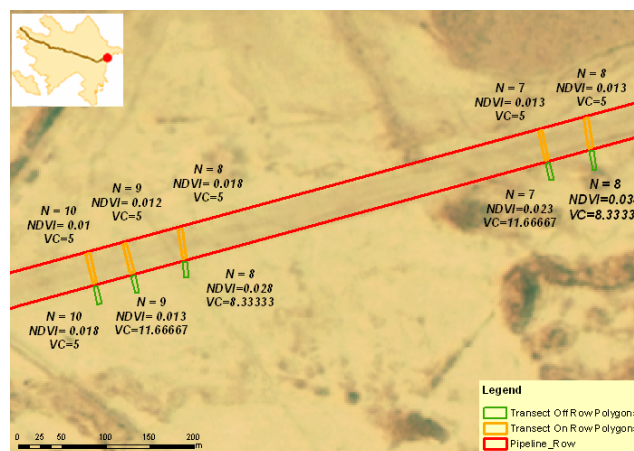


**Figure 3.17: Sample transects' polygons with extracted NDVI from FORMOSAT NDVI spatial grids and with field measured Vegetation Cover for 2008 (backdrop – FORMOSAT)**

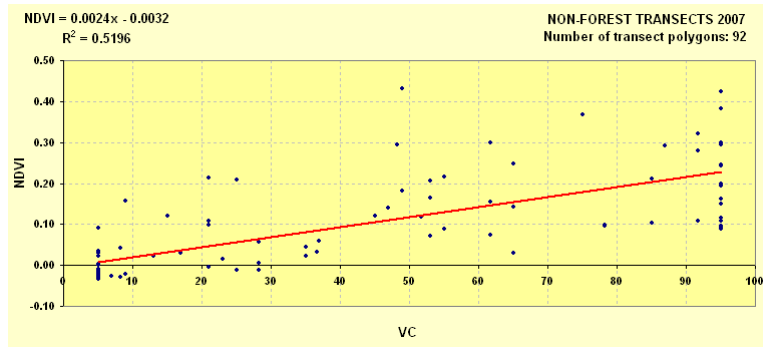


**Figure 3.18: Regression between Transects' NDVI 2007 and field measured Vegetation Cover 2007 for these transects within non-forest habitat for entire pipeline route.**

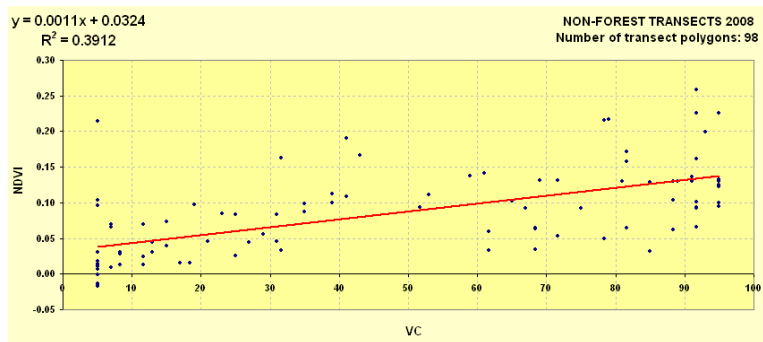


**Figure 3.19: Regression between Transects' NDVI 2008 and field measured Vegetation Cover 2008 for these transects within non-forest habitat for entire pipeline route.**

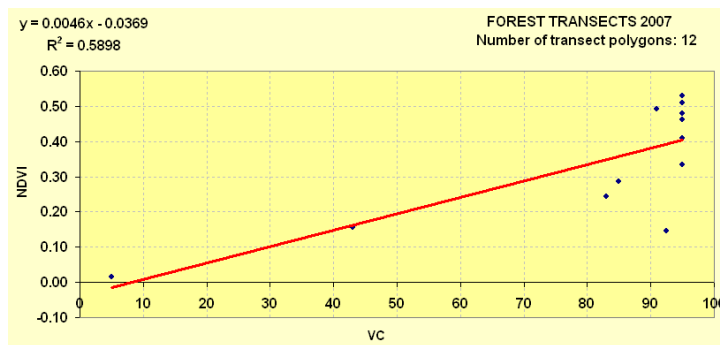


**Figure 3.20: Regression between Transects' NDVI 2007 and field measured Vegetation Cover 2007 for these transects within forest habitat for entire pipeline route.**

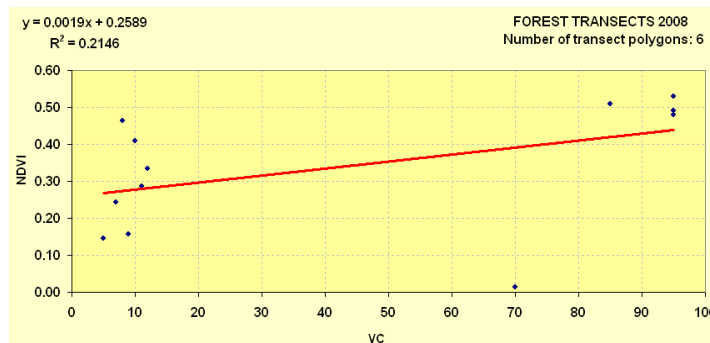


**Figure 3.21: Regression between Transects' NDVI 2008 and field measured Vegetation Cover 2008 for these transects within forest habitat for entire pipeline route.**

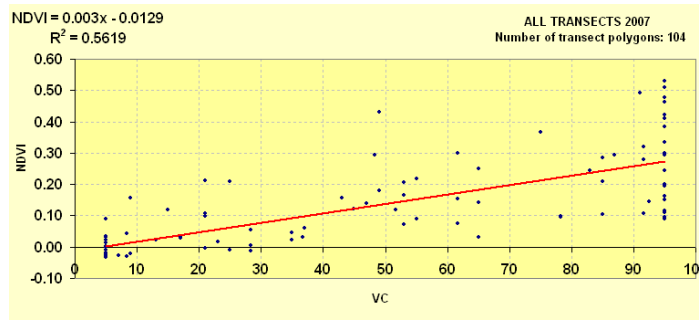


**Figure 3.22: Regression between Transects' NDVI 2007 and field measured Vegetation Cover 2007 for these transects within general habitat for entire pipeline route.**

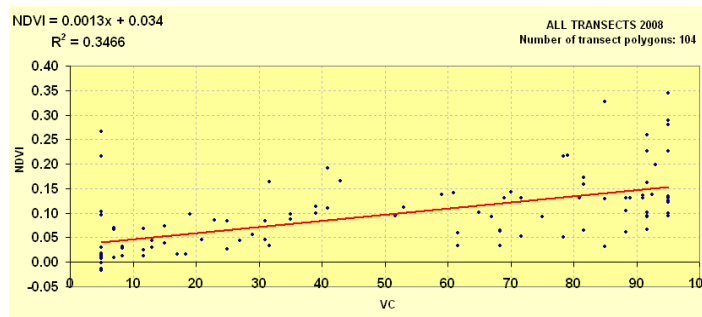


**Figure 3.23: Regression between Transects' NDVI 2008 and field measured Vegetation Cover 2008 for these transects within general habitat for entire pipeline route.**

### 3.7. Vegetation Cover Spatial Grids

Based on the acquired equations for non-forest and forest habitat (Figure 3.18, 3.19, 3.20, 3.21), NDVI spatial grids 2007 (IKONOS) and NDVI spatial grids 2008 (FORMOSAT) of pipeline route were recalculated to spatial grids of vegetation cover 2007 and 2008. Recalculation was achieved for the entire pipeline route and two example areas are presented on Figure 3.24, 3.25, 3.26, 3.27 for 2007 and 2008 Spatial Grids of Vegetation Cover. This recalculation allowed turning from NDVI units of measurement to Vegetation Cover percentage and at the same time to normalize NDVI 2007 acquired from IKONOS and NDVI 2008 acquired from FORMOSAT to ground truth situation using data from field transects' vegetation cover measurements.



Figure 3.24: Calculated Vegetation Cover spatial grid 2007 from NDVI spatial grid 2007 for sample area 1 (Backdrop – IKONOS image).



Figure 3.25: Calculated Vegetation Cover spatial grid 2008 from NDVI spatial grid 2008 for sample area 1 (Backdrop – FORMOSAT image).

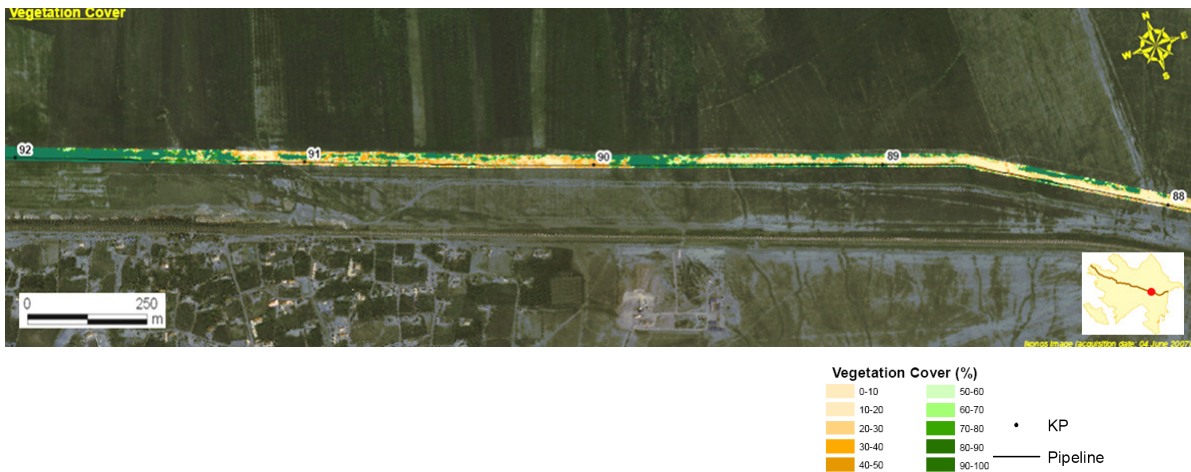
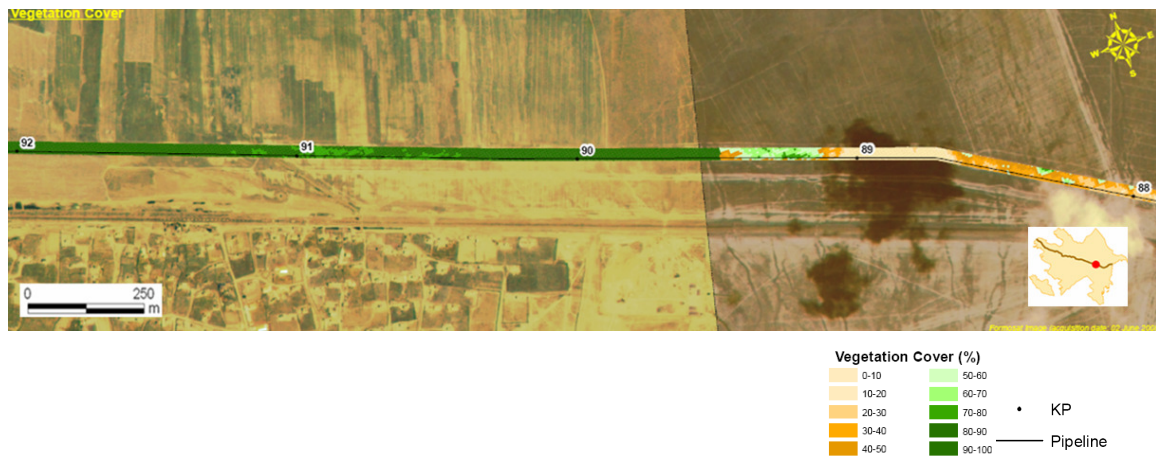


Figure 3.26: Calculated Vegetation Cover spatial grid 2007 from NDVI spatial grid 2007 for sample area 2 (Backdrop – IKONOS image)



**Figure 3.27: Calculated Vegetation Cover spatial grid 2008 from NDVI spatial grid 2008 for sample area 2 (Backdrop – FORMOSAT image)**

### 3.8. Geostatistical analysis results of vegetation cover grids

As a result, Vegetation Cover spatial grids for 2007 and 2008 allowed to develop the graphs of vegetation cover to determine areas belonging to each percentage of vegetation cover along pipeline route (Figure 3.28, 3.29). For instance, the area of 20-30% vegetation cover along pipeline route was 375160 sq. m. in 2007 (Figure 3.28) but in 2008 it improved to 421000 sq. m (Figure 3.29). At the same time it is possible to observe that 0-10% class reduced in area in 2008 since some other percentage classes increased in vegetation cover (Figure 3.28, 3.29). 90-100% was 923036 sq. m in 2007 since bio-restoration activities started earlier (after pipeline construction completion in 2005) and as a result in 2008 it became 990000 sq. m. what means that some amount of vegetation cover from lower percentage classes reached 90-100%.

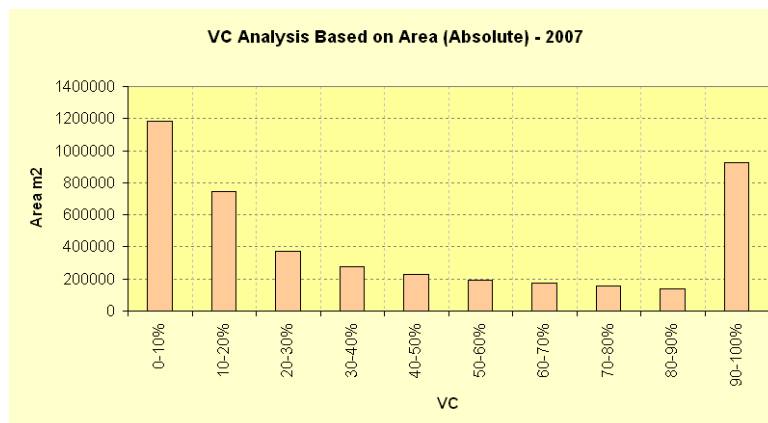


**Figure 3.28: Percentage of Vegetation Cover distribution in 2007 along entire pipeline route**

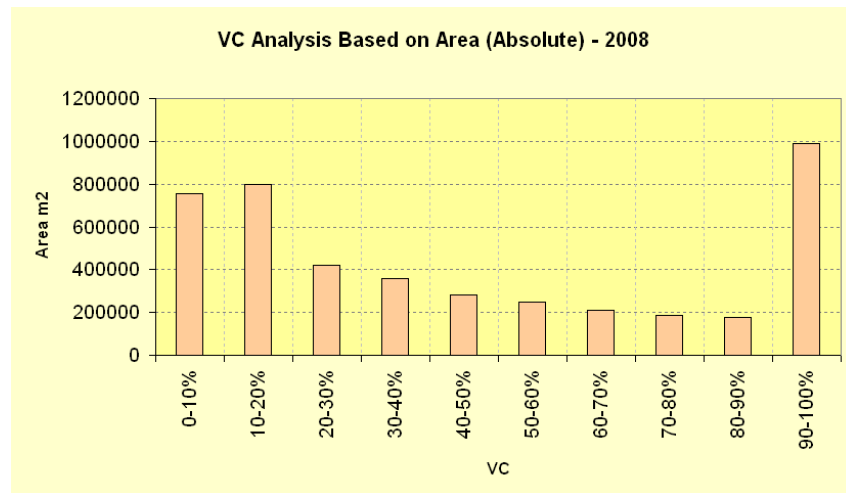


Figure 3.29: Percentage of Vegetation Cover distribution in 2008 along entire pipeline route

### 3.9. Spatial grid of NDVI gain coefficients

Stage for the calculation of spatial grids with gain coefficients which define annual re-growth to each pixel, resulted in a visual representation of areas with negative and positive vegetation cover re-growth status between 2007 and 2008. For this stage it was applied to NDVI spatial grids 2007 from IKONOS and NDVI spatial grid 2008 from FORMOSAT since they are original sources of spatial grids to develop and analyze the spatial grids of NDVI gain coefficients. Resulted spatial grids of gain coefficients are presented for areas 1 and 2 along pipeline corridor (Figure 3.30, 3.31).

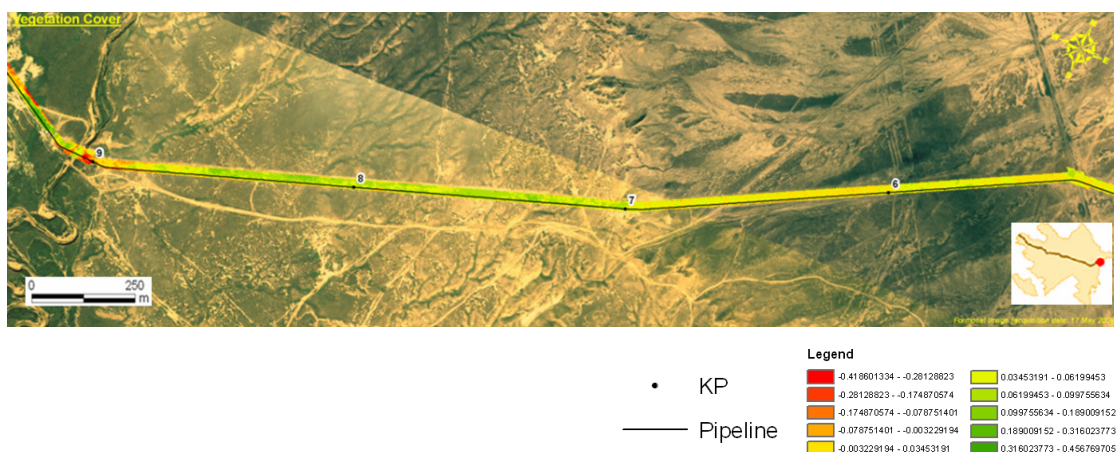


Figure 3.30: Spatial grid of gain coefficients between 2007 and 2008 for sample area 1

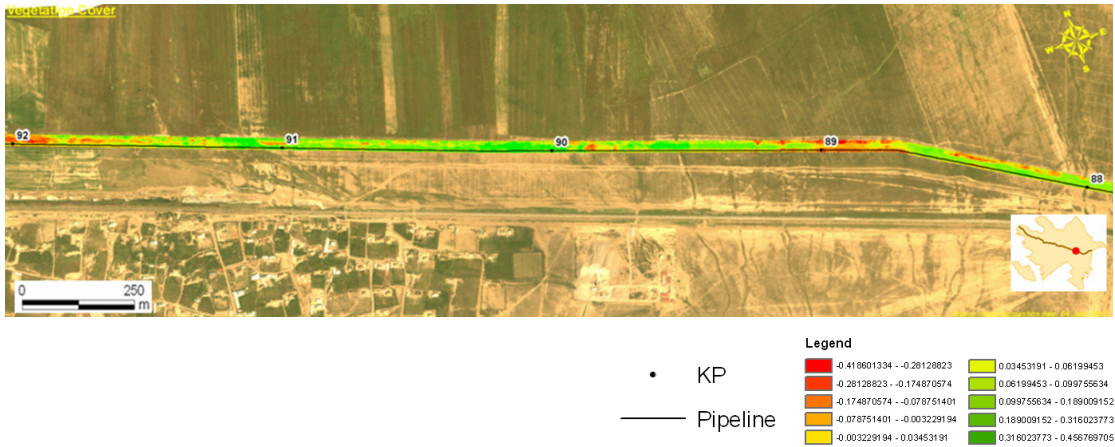


Figure 3.31: Spatial grid of gain coefficients between 2007 and 2008 for sample area 2

### 3.10. Re-growth status of On RoW Vegetation cover relative to Off RoW

As a result of the last stage for determination of On RoW vegetation status relative to Off RoW, it was calculated relative re-growth of On RoW to Off RoW vegetation cover since one of the objectives of biorestore activities is to achieve the same vegetation cover status for On RoW as it is for Off RoW where vegetation cover was not disturbed during construction process.

Based on the divided pipeline On RoW corridor into 100 m polygons and adjacent 10 m diameter polygonal circles along Off RoW pipeline area from both sides of 100 m polygons (Figure 3.32, Figure 3.33), mean NDVI were extracted for both 100 m polygons and 10 m polygonal circles from NDVI 2007 and NDVI 2008 spatial grids and this allowed to make statistical calculation of vegetation cover relative re-growth of On RoW to Off RoW (Figure 2.13, Formula 4, 5) and the achieved result is represented on Table 3.5 and Figure 3.34.

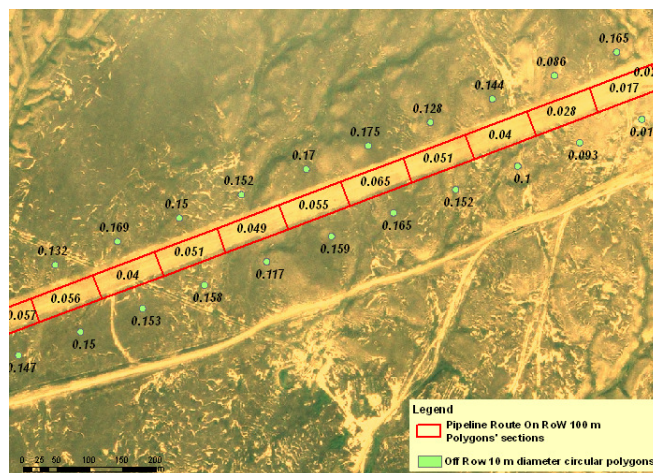
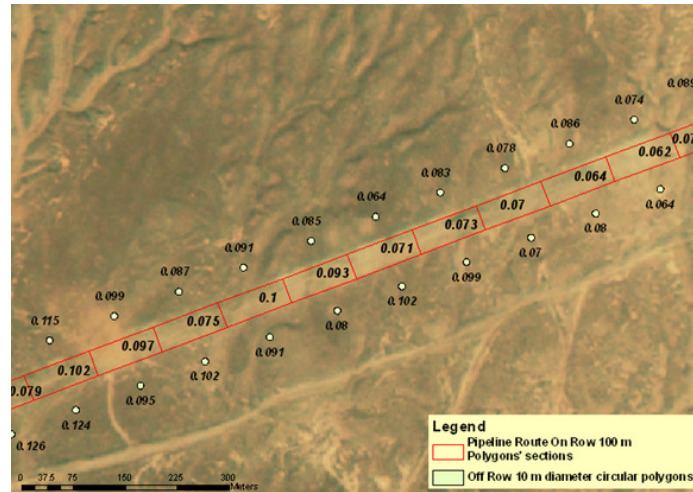


Figure 3.32: On RoW 100 m polygons and Off RoW 10 m diameter circular polygons with extracted NDVI values from 2007 NDVI Spatial Grid of IKONOS





**Figure 3.33: On RoW 100 m polygons and Off RoW 10 m diameter circular polygons with extracted NDVI values from 2008 NDVI Spatial Grid of FORMOSAT**

As it is represented on Table 3.5 and Figure 3.34, re-growth status of On RoW vegetation cover relative to Off RoW is successful since most of positive re-growth percentage classes contain significant number of 100 m pipeline corridor polygons.

**Table 3.5: Number of On RoW 100 m Polygons and percent of these polygons relative to re-growth classes**

Classes	Number of On RoW Polygons of 100m	Percent (%) of On RoW Polygons of 100m
(-100) - (- 90)	5	0.438
(-90) - (-80)	11	0.963
(-80) - (- 70)	10	0.876
(-70) - (- 60)	7	0.613
(-60) - (- 50)	12	1.051
(-50) - (- 40)	14	1.226
(-40) - (- 30)	25	2.189
(-30) - (- 20)	22	1.926
(-20) - (- 10)	26	2.277
(-10) - (0)	70	6.13
0 - 10	155	13.573
10 - 20	130	11.384
20 - 30	100	8.757
30 - 40	95	8.319
40 - 50	80	7.005
50 - 60	65	5.692
60 - 70	55	4.811
70 - 80	50	4.378
80 - 90	47	4.116
90 - 100	48	4.203
>100	111	10.073
	1138	100

Based on the Table 3.5, the Figure 3.34 was generated and it represents the re-growth of On RoW vegetation cover relative to Off RoW.

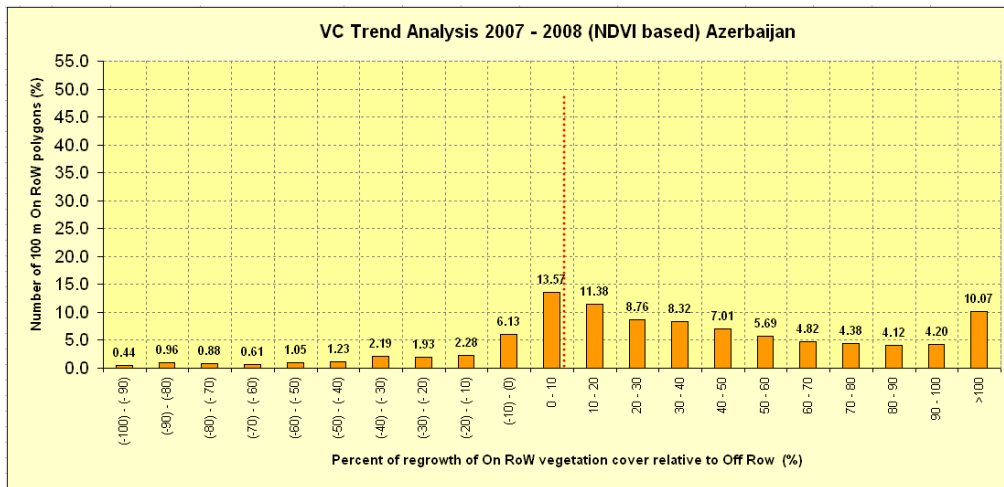


Figure 3.34: Vegetation cover re-growth of On RoW relative to Off RoW between 2007 and 2008

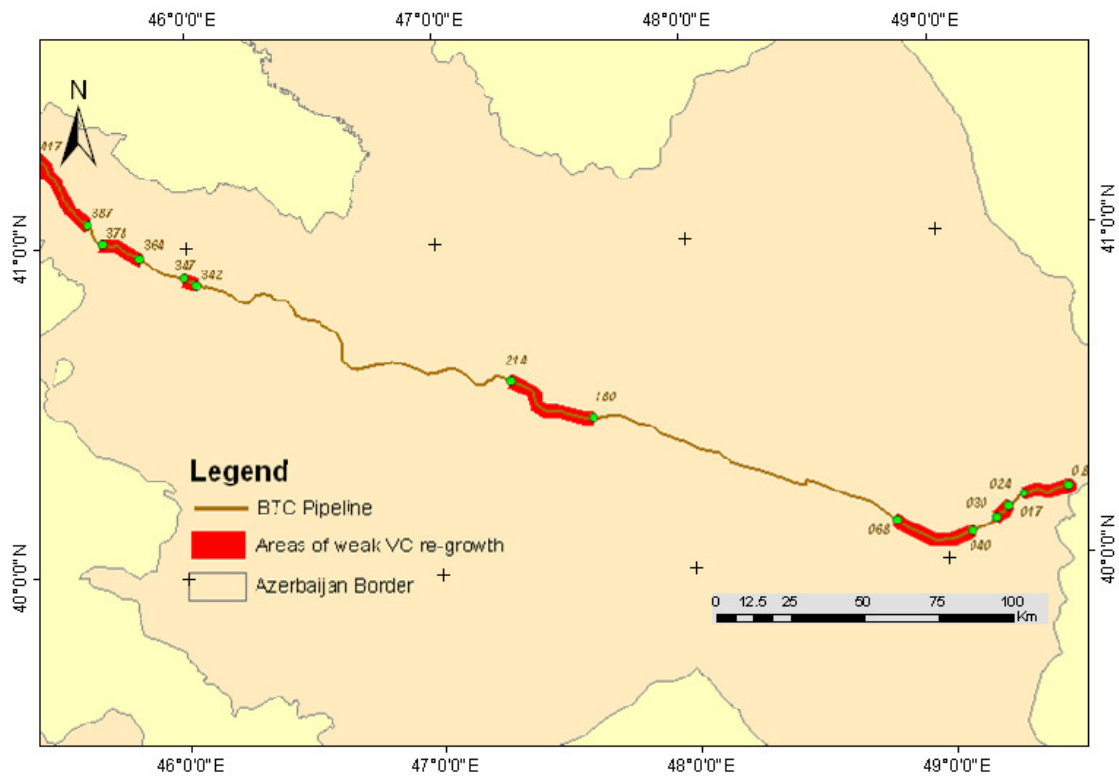


Figure 3.35: Areas of weak vegetation cover re-growth along pipeline with a demand for continuation of bio-restoration activities in 2009

## **DISCUSSION**

### **4.1 Photogrammetric processing of satellite images**

All high resolution multispectral satellite images of 2007 and 2008 along pipeline route were geometrically corrected and RMSE achieved for each image was up-to +/- 2 m. The positional accuracy plays important role when it is dealt with detailed level of territorial analysis. One of the significant factors for achievement of reliable results in GIS and Remote Sensing analysis on the detailed level is accurate overlaying of remotely sensed data from various sensors and supplementary ground truth information.

For the achievement of appropriate positional accuracy of satellite images along pipeline corridor, polynomial coefficients of images, rational distribution of GCP and accurate DEM and analytical analysis of triangulation results were the most important factors in this geometrical correction process.

### **4.2 GIS and Remote Sensing processing**

The results of NDVI to Vegetation Cover recalculation allowed calibrating satellite images to ground truth situation and at the same time to move from NDVI units to the classified units of vegetation cover. Transects, rationally distributed for each habitat along pipeline, had differences in the field collection period relative to the acquisition of satellite images that's why appropriate corrections using theoretical re-growth graphs of different habitats along pipeline route were applied to bring the level of measured vegetation cover for transects to the date of images acquisition. Because of temporal factors negatively affected (Yuanbo, et al, 2005) to FORMOSAT 2008 images in two areas (Figure 3.8), NDVI spatial grids derived from FORMOSAT 2008 image for these two areas (Figure 3.8) were normalized to the NDVI of baseline high spectral and spatial resolution IKONOS 2007 images using NDVI values from Off RoW areas with non-disturbed vegetation so that not to negatively affect to NDVI spatial grids extracted from FORMOSAT images. The correlation of required areas along Off RoW between NDVI spatial grids from IKONOS 2007 and FORMOSAT 2008 were reaching up-to 50% (Figure 3.9, 3.10). It could also be possible to apply to some atmospheric corrections for FORMOSAT images but it could negatively affect

to NDVI spatial grids from FORMOSAT images since this sensor model appeared in 2004 and not completely studied to consider all corrections to temporal factors.

NDVI spatial grids acquired from IKONOS 2007 and FORMOSAT 2008 images were applied for the regression with collected transects' vegetation cover values of 2007 and 2008 correspondingly (Figure 3.18, 3.19, 3.20, 3.21, 3.22, 3.23). This allowed recalculating NDVI to vegetation cover spatial grids and based on the achieved results of recalculation it was possible to develop maps of vegetation cover percentage classes and to evaluate qualitatively and quantitatively vegetation cover of 2007 and 2008 along entire pipeline corridor (Figure 3.28, 3.29).

To evaluate areas along pipeline corridor regarding status of vegetation cover re-growth it was developed the maps of NDVI gain coefficients showing annual re-growth between 2007 and 2008 and the analysis of re-growth allowed to identify areas with positive and negative re-growth. For instance, areas with weak vegetation cover re-growth on Figure 3.34 show necessity for the continuation of bio-restoration activities in the specific areas of pipeline corridor.

Evaluation of relative re-growth of On RoW to Off RoW vegetation cover presented the positive trend of On RoW vegetation cover in reaching of adjacent non-disturbed Off RoW vegetation cover status (Figure 3.34).

### **4.3 GIS and Remote Sensing in bio-restoration activities and practicality of achieved results for oil and gas field**

Bio-restoration activities are required along pipeline corridor to establish sufficient vegetation cover to reduce erosion and loss of fertile and productive topsoil layers, reinstate the variety and distribution pattern of the original plant species with the long-term objective to restore the land to condition that is equal to or an enhancement of the pre-disturbed state and generally for re-establishment of ecosystems. Bio-restoration activities should be well planned before starting them and monitored consequently. For bio-restoration activities of such territorial range and detailed level requires GIS based collaborative environmental management approach to plan all activities focused on bio-restoration. The process of bio-restoration should be measurable to achieve successful results through environmental monitoring of negative or positive change dynamics. It is also necessary to define in advance the criteria how to measure the success of bio-restorations activities.

GIS and Remote Sensing in integration, play important role for the implementation of such collaborative environmental management and decision support systems involving a lot of stakeholders like geographers, environmentalists and biologists etc. to participate efficiently in this process and monitor it.

GIS and Remote Sensing results of this research provided the base for the continuation of bio-restoration activities and allowed to plan bio-restoration activities by determination of areas of interest for 2009 (Figure 3.35). Along with the application of achieved results for vegetation cover restoration monitoring as it is presented in this research, they can be applied for the assessment of potential erosion areas along pipeline route and this will allow planning of geotechnical works (Morgan, et al, 2003; Hann, et al, 2006). The role of GIS and Remote Sensing will be crucial in the implementation of these works.

#### **4.4 Critical Issues of the developed methodology and recommendations**

The discussions are required for the critical issues negatively affecting to the developed methodology and for the recommendations and they are following:

##### 1. Differences in sensors of acquired satellite images

Environmental monitoring of pipeline corridor required two sets of data for 2007 and 2008. In 2007, it was possible to acquire IKONOS 2007 images but in 2008 it was only possible to acquire FORMOSAT 2008. In comparison of spatial and spectral characteristic of FORMOSAT 2008 to IKONOS 2007 images, IKONOS images hold higher spectral and spatial properties. Since similar research works require high quality of NDVI with high spatial resolution it is preferable to select the images with the highest capacity and at the same time it is preferable to apply to the images coming from the same sensor to have the same spatial and spectral resolution. This factor is crucial to avoid of errors raised from images acquired from different sensors.

##### 2. Excessive human being dependent factors

Evaluation of vegetation cover in 2007 and 2008 required a lot of human intervention through the approximate evaluation by the way of quadrates what is also a negative factor raising the errors. Moreover, the work of transects' collection and evaluation of vegetation cover are recourse and time consuming, that's why most time it ends up with a lower number of collected transects than is required.

##### 3. Low correlation between NDVI and vegetation cover values in 2007 and 2008

The total pipeline corridor is 442 km with rationally distributed 53 transects along it. Since the equation for the recalculation of NDVI to vegetation cover was achieved for

the entire pipeline corridor, the regression coefficient was up-to 50% that is not so high. To achieve higher regression coefficient it would be more reasonable to conduct regression for the different sections of pipeline separately, but this would require higher number of transects.

Both NDVI derived from IKONOS 2007 and FORMOSAT 2008 satellite images showed up-to 50% regression with the transects' vegetation cover values what is not so high than it was expected that's why after recalculation of NDVI spatial grids to vegetation cover grids, it is inevitable to control the quality of achieved results by using applied and additional "check" transects to asses difference between vegetation cover values derived from vegetation cover spatial grids and field evaluated transects. Satellite images along pipeline should be also colour-balanced to natural colours so that to partly asses the achieved vegetation cover spatial grid over the background images. It is also necessary to apply to the collection of census by questionnaires provided to the end-users conducting bio-restoration in order to gather information regarding practicality of the produced vegetation cover and re-growth maps in the field conditions for re-vegetation activities and to get their feedbacks.

#### 4. Differences in periods of acquired images and ground truth data

During the research some transects in 2008 had the differences for the dates of collection with the dates of satellite images acquisition for those areas. That is why it was necessary to apply to the theoretical On RoW and Off RoW re-growth curves of specific habitats to normalize field collected vegetation cover values of transects to vegetation cover values corresponding to the dates of their acquired satellite images. This is the most error raising way of solution since the theoretical re-growth curves (Figure 2.11) hold only a theoretical character. Moreover vegetation cover re-growth curve is not the same every year because of natural variations and this may yield serious errors to ground truth data what in its turn will be negatively expressed in the regression analysis.

#### 5. Low spatial resolution of multispectral bands for the pipeline corridor

The multispectral bands of IKONOS were 4 m and of FORMOSAT were 8 m. The pan-sharpening process increases the spatial resolution but doesn't make any positive impact on the multispectral quality of images (ERDAS Field Guide, 2005), that's why it necessary to rely only to the NDVI outcomes from the original multispectral bands. The pipeline corridor is 44 m and within this corridor it is possible to fit 11 pixels coming from IKONOS NDVI spatial grid and 5.5 pixels coming from FORMOSAT

NDVI spatial grid. This amount of pixels with multispectral properties practically is not so sufficient for the achievement of high regression results between remotely sensed and ground truth data.

#### 6. Lack of knowledge in atmospheric corrections

Some of FORMOSAT images acquired in 2008 were affected to atmospheric distortions but because this satellite started functioning in 2004, there is still lack of existing algorithms specialized for FORMOSAT images to apply atmospheric correction for the normalization requiring FORMOSAT images before generation NDVI spatial grids.

#### 7. Lack of knowledge in removing of negative temporal factors affected on satellite images

Some of FORMOSAT images acquired in 2008 were affected to temporal factors and this issue was partly solved by normalization of some FORMOSAT NDVI spatial grids to IKONOS NDVI spatial grids by generated points along Off RoW (Figure 3.32, 3.33). This was certainly not the most correct way as a solution to this problem since the vegetation cover along Off RoW areas along pipeline corridor between 2007 and 2008 might be significantly affected by natural variations. It is necessary to research deeply on how to remove negative effects of temporal factors from FORMOSAT images before calculation of NDVI.

#### 8. Lack of data for quality control

The similar works should be accompanied by the collection of data for the quality control of the final products. The quality control can be feasible in combination of 4 following sources: applied and additional “check transect”, census from end-users regarding the quality, involvement of some other data sources and partly using colour balanced satellite images as a backdrop. Unfortunately because of lack of data in this research and in particular non-availability of “check” transects, it was not possible to completely control the final results.

## **CONCLUSION**

This research allowed making overall analysis of bio-restoration activities along Azerbaijan BTC pipeline between 2007 and 2008 years using Geographical Information Systems (GIS), Remote Sensing and Photogrammetry methods. These methods gave a possibility to determine vegetation cover and its re-growth using developed NDVI from geometrically corrected high resolution multispectral IKONOS and FORMOSAT satellite images and transects collected along pipeline corridor.

Conducted research laid out the base for determination of areas with negative and positive bio-restoration results during the period of research and to plan further areas along pipeline for the continuation of reinstatement works.

The developed methodology gives possibility for restoration of nature during collaborative environmental management in the oil and gas and other fields using GIS and Remote Sensing not only in Azerbaijan but also in other countries.



## REFERENCES

1. AETC (Azerbaijan Environment and Technology Centre) Ltd/ERM, 2002. Environmental and Social Impact Assessment Report, Baku-Tbilisi-Ceyhan, Azerbaijan.
2. Aliyev F., Muller H., Salmanova L., Bayramov E., 2006. Azerbaijan – The Land of Incomparable Nature, 213 p.
3. Amini J., Hashemi A. R. M., 2005. From Pharaohs to Geoinformatics FIG Working Week and GSDI-8, Cairo, Egypt, 20.
4. Atlas of Azerbaijan Republic, 1979. Baku, Azerbaijan, 213p.
5. Bayramov E. R., Bayramov, R.V., 2004. Preparation of Orthophotos from IKONOS Imagery for Cadastre Base Mapping of Nakhchevan Autonomous Republic Territory, In: Proceedings of ISPRS XXXV Congress, 12-23 July 2004 Turkey, Istanbul, 21-22.
6. Bayramov, E. R., 2007. Up-to-date GIS based method as the important component of Landscape Planning to predict Caspian water level fluctuation impacts on the located along Caspian Sea Coastal Line Natural Protected Areas, This paper appears in: Recent Advances in Space Technologies, RAST '07. 3rd International Conference, Istanbul, Turkey, 256-258.
7. Bayramov, E. R., Mamedov, R., 2008. GIS based Landscape and Environmental Planning Instrument for the Azerbaijan Caspian Sea Coastal Nature Protected Areas, Proceedings of ESRI Federal User Conference, Washington, D.C.
8. Bayramov, E.R., Mamedov, R., 2008. Modelling Method for the Prediction of the Caspian Sea Level Fluctuation Impacts on the Azerbaijan Coastal Zones Landscape Based on GIS Ekoloji, 17, 67, 46-51
9. Bayramov, E., Mamedov, R., Ismayilov, J., 2006. Up-to-date method for the definition of the variability areas on the different levels of the Caspian sea coastal zones, Caspian Region: Scientific Journal “Caspian: right, economy, culture”, Astrakhan, 2, 9,14-17.
10. Bechtel A., Puttmann W., Carlson T.N., and Ripley D.A. 1997. On the Relation between NDVI, Fractional Vegetation Cover, and Leaf Area Index. Remote Sensing of Environment, 62, No 3, 241-252.

11. ERDAS Field Guide, 2005, Leica Geosystems Geospatial Imaging, LLC, USA, 698p.
12. Hann M. J. and Morgan R. P. C., 2006, Evaluating erosion control measures for biorestorement between the time of soil reinstatement and vegetation establishment, *Earth Surface Processes and Landforms*, 31, 589–597
13. Hong G., Zhang Y., 2007, A comparative study on radiometric normalization using high resolution satellite images, *International Journal of Remote Sensing*, 29:2, 425-438
14. Huete A.R., Liu H., 1994. An error and sensitivity analysis of the atmospheric- and soil-correcting variants of the NDVI for the MODIS-EOS. *IEEE Transactions on Geoscience and Remote Sensing*, 32, 897–905.
15. IKONOS Sensor Model Support Tour Guide, 2003, Leica Geosystems GIS&Mapping, LLC, USA, 68p.
16. Leprieur, C., Kerr, Y.H., Mastorchio, S. and Meunier, J.C., 2000. Monitoring vegetation cover across semi-arid regions: Comparison of remote observations from various scales. *International Journal of Remote Sensing*, 21, 281–300.
17. Liang-Chien C., Tee-Ann T., and Chien-Liang L., 2006. The Geometrical Comparisons of RSM and RFM for FORMOSAT-2 Satellite Images. *Photogrammetric Engineering & Remote Sensing*, 72, No.5, 573-579.
18. Liu, S.J., Tong, X.H., 2008. Transformation between rational function model and rigorous sensor model for high resolution satellite imagery, the *International Archives of the Photogrammetry. Remote Sensing and Spatial Information Sciences*, XXXVII. Part B1, 873-877.
19. Morgan R.P.C., Mirtskhoulava Ts.E., Nadirashvili V., Hann1 M.J., Gasca A.H., 2003, Spacing of Berms for Erosion Control along Pipeline Rights-of-way, *Biosystems Engineering*, 85 (2), 249–259
20. Yuanbo L., Hiyama, T., Yamaguchi, Y., Kimura, R., Nishiyama, S., 2005, Effect of temporal factors on satellite image in reflective band: a simulation with regard to change detection, 3, 2125-2128

## APPENDIX 1, Table of Transect's list with Vegetation Cover and mean NDVI

TRANSECT	HABITAT	NDVI2007	NDVI2008	ROW	VC2007	VC2008
AZ-1	Suaedetum microphylla solonchak desert	-0.0292	0.0100	1	8.3333	8.3333
AZ-1	Suaedetum microphylla solonchak desert	-0.0319	-0.0100	2	5.0000	5.0000
AZ-2	Halocnemetum strobilaceum solonchak desert	-0.0281	0.0050	1	5.0000	5.0000
AZ-2	Halocnemetum strobilaceum solonchak desert	-0.0336	-0.0240	2	5.0000	5.0000
AZ-3	Halocnemetum strobilaceum solonchak desert	-0.0300	0.0090	1	5.0000	5.0000
AZ-3	Halocnemetum strobilaceum solonchak desert	-0.0305	-0.0010	2	5.0000	5.0000
AZ-4	Halocnemetum strobilaceum solonchak desert	-0.0101	0.0160	1	5.0000	5.0000
AZ-4	Halocnemetum strobilaceum solonchak desert	-0.0290	0.0120	2	5.0000	5.0000
AZ-5	Halocnemetum strobilaceum solonchak desert	0.2942	0.0160	1	48.3333	18.3333
AZ-5	Halocnemetum strobilaceum solonchak desert	-0.0194	0.0090	2	5.0000	7.0000
AZ-6	Suaedetum microphylla solonchak desert	0.0318	0.0340	1	36.6667	8.3333
AZ-6	Suaedetum microphylla solonchak desert	-0.0267	0.0130	2	5.0000	5.0000
AZ-7	Suaedetum microphylla solonchak desert	0.0217	0.0230	1	35.0000	11.6667
AZ-7	Suaedetum microphylla solonchak desert	-0.0221	0.0130	2	9.0000	5.0000
AZ-8	Salsoletum dendroides clayey desert	0.0064	0.0280	1	28.3333	8.3333
AZ-8	Salsoletum dendroides clayey desert	-0.0272	0.0180	2	7.0000	5.0000
AZ-9	Salsoletum dendroides clayey desert	-0.0215	0.0130	1	5.0000	11.6667
AZ-9	Salsoletum dendroides clayey desert	-0.0219	0.0120	2	5.0000	5.0000
AZ-10	Salsoletum dendroides clayey desert	-0.0175	0.0180	1	5.0000	5.0000
AZ-10	Salsoletum dendroides clayey desert	-0.0266	0.0100	2	5.0000	5.0000
AZ-11	Artemisetum lerchiana clayey desert	0.1507	0.0320	1	95.0000	85.0000
AZ-11	Artemisetum lerchiana clayey desert	0.0305	0.0440	2	5.0000	13.0000
AZ-12	Salsoletum nodulosae clayey desert	0.2455	0.1040	1	95.0000	88.3333
AZ-12	Salsoletum nodulosae clayey desert	0.1577	0.0970	2	9.0000	19.0000
AZ-13	Salsoletum nodulosae clayey desert	0.0865	0.1050	1	95.0000	95.0000
AZ-13	Salsoletum nodulosae clayey desert	0.0771	0.1040	2	5.0000	5.0000
AZ-14	Salsoletum nodulosae clayey desert	0.1538	0.0960	1	51.6667	35.0000
AZ-14	Salsoletum nodulosae clayey desert	0.0724	0.0990	2	5.0000	39.0000
AZ-15	Salsoletum nodulosae clayey desert	0.0238	0.0920	1	95.0000	91.6667
AZ-15	Salsoletum nodulosae clayey desert	0.0225	0.0960	2	5.0000	5.0000
AZ-16	Artemisetum lerchiana clayey desert	0.1088	0.1000	1	95.0000	95.0000
AZ-16	Artemisetum lerchiana clayey desert	0.0906	0.0880	2	5.0000	35.0000
AZ-17	Salsoletum nodulosae clayey desert	0.0962	0.0660	1	78.3333	68.3333
AZ-17	Salsoletum nodulosae clayey desert	0.0001	0.0740	2	5.0000	15.0000
AZ-18	Salsoletum nodulosae clayey desert	0.1148	0.0570	1	95.0000	71.6667
AZ-18	Salsoletum nodulosae clayey desert	-0.0108	0.0630	2	25.0000	29.0000
AZ-19	Ephemeral desert	0.0980	0.0630	1	78.3333	68.3333
AZ-19	Ephemeral desert	-0.0098	0.0700	2	5.0000	7.0000
AZ-20	Ephemeral desert	0.0947	0.0630	1	95.0000	81.6667
AZ-20	Ephemeral desert	-0.0096	0.0860	2	5.0000	25.0000
AZ-21	Ephemeral desert	0.0890	0.0890	1	95.0000	51.6667
AZ-21	Ephemeral desert	-0.0089	0.0840	2	5.0000	23.0000
AZ-22	Salsoletum dendroides clayey desert	0.1944	0.1590	1	95.0000	91.6667
AZ-22	Salsoletum dendroides clayey desert	0.0322	0.1420	2	17.0000	61.0000
AZ-23	Artemisetum lerchiana clayey desert	0.1418	0.1720	1	65.0000	81.6667
AZ-23	Artemisetum lerchiana clayey desert	0.0348	0.1090	2	5.0000	41.0000
AZ-27	Chal meadow	0.1070	0.2260	1	91.6667	91.6667
AZ-27	Chal meadow	0.0235	0.1910	2	5.0000	41.0000
AZ-28	Chal meadow	0.1176	0.2160	1	51.6667	78.3333
AZ-28	Chal meadow	0.0301	0.2150	2	5.0000	5.0000

AZ-29	Capparisetum spinosa clayey desert	0.1038	0.0430	1	85.0000	15.0000
AZ-29	Capparisetum spinosa clayey desert	0.0288	0.0460	2	17.0000	31.0000
AZ-30	Capparisetum spinosa clayey desert	0.0557	0.0330	1	28.3333	31.6667
AZ-30	Capparisetum spinosa clayey desert	0.0025	0.0260	2	5.0000	25.0000
AZ-31	Capparisetum spinosa clayey desert	0.0456	0.0690	1	35.0000	11.6667
AZ-31	Capparisetum spinosa clayey desert	0.0156	0.0160	2	23.0000	17.0000
AZ-32	Halocnemetum strobilaceum solonchak desert	0.0426	0.0340	1	8.3333	68.3333
AZ-32	Halocnemetum strobilaceum solonchak desert	-0.0237	0.0300	2	5.0000	5.0000
AZ-33	Tamarixetum scrub	0.0145	0.1540	2	5.0000	70.0000
AZ-33	Tamarixetum scrub	0.1463	0.2610	1	92.5000	5.0000
AZ-34	Halocnemetum strobilaceum solonchak desert	0.0307	0.0600	1	65.0000	61.6667
AZ-34	Halocnemetum strobilaceum solonchak desert	-0.0208	0.0460	2	5.0000	21.0000
AZ-35	Tugay forest (East)	0.4918	0.2880	2	91.0000	95.0000
AZ-35	Tugay forest (East)	0.5096	0.3330	1	95.0000	85.0000
AZ-36	Tugay forest (East)	0.5297	0.2930	2	95.0000	95.0000
AZ-36	Tugay forest (East)	0.4787	0.3460	1	95.0000	95.0000
AZ-37	Halocnemetum strobilaceum solonchak desert	-0.0130	0.0310	1	28.3333	61.6667
AZ-37	Halocnemetum strobilaceum solonchak desert	-0.0336	0.0330	2	5.0000	13.0000
AZ-38	Halocnemetum strobilaceum solonchak desert	0.0747	0.0430	1	61.6667	78.3333
AZ-38	Halocnemetum strobilaceum solonchak desert	0.0223	0.0500	2	13.0000	27.0000
AZ-41	Phragmiteta - typhetum marsh	0.2990	0.1250	1	95.0000	95.0000
AZ-41	Phragmiteta - typhetum marsh	0.4315	0.1220	2	49.0000	95.0000
AZ-42	Phragmiteta - typhetum marsh	0.3205	0.1290	1	91.6667	85.0000
AZ-42	Phragmiteta - typhetum marsh	0.2062	0.1310	2	52.5000	69.0000
AZ-43	Artemisetum botriochloasum semidesert	0.1612	0.2750	1	95.0000	95.0000
AZ-43	Artemisetum botriochloasum semidesert	0.1082	0.2750	2	21.0000	65.0000
AZ-44	Artemisetum botriochloasum semidesert	0.2489	0.2750	1	65.0000	71.6667
AZ-44	Artemisetum botriochloasum semidesert	0.1211	0.2750	2	45.0000	53.0000
AZ-45	Artemisetum botriochloasum semidesert	0.2989	0.2760	1	61.6667	81.6667
AZ-45	Artemisetum botriochloasum semidesert	0.0975	0.2760	2	21.0000	43.0000
AZ-52	Artemisetum botriochloasum semidesert	0.2125	0.2750	1	95.0000	95.0000
AZ-52	Artemisetum botriochloasum semidesert	0.1549	0.2750	2	93.0000	91.0000
AZ-46	Artemisetum botriochloasum semidesert	0.2093	0.2760	1	25.0000	31.6667
AZ-46	Artemisetum botriochloasum semidesert	0.0721	0.2750	2	45.0000	59.0000
AZ-47	Tamarixetum scrub	0.0000	0.2560	1	95.0000	92.5000
AZ-47	Tamarixetum scrub	0.0000	0.2410	2	85.0000	95.0000
AZ-48	Artemisetum lerchiana purum desert	0.1657	0.2240	2	53.0000	81.0000
AZ-48	Artemisetum lerchiana purum desert	0.2951	0.2250	1	95.0000	95.0000
AZ-49	Artemisetum lerchiana purum desert	0.4235	0.2300	1	95.0000	95.0000
AZ-50	Artemisetum lerchiana purum desert	0.2927	0.2260	2	75.0000	89.0000
AZ-50	Artemisetum lerchiana purum desert	0.3834	0.2250	1	95.0000	88.3333
AZ-49	Artemisetum lerchiana purum desert	0.3679	0.2260	2	87.0000	91.0000
AZ-53	Temporary soil storage	0.2103	0.2750	1	85.0000	75.0000
AZ-53	Temporary soil storage	0.1398	0.2750	2	47.0000	67.0000
AZ-55	Spoil Pit	0.1992	0.2210	1	95.0000	91.6667
AZ-55	Spoil Pit	0.1197	0.2230	2	15.0000	39.0000
AZ-56	Spoil Pit	0.1614	0.0900	1	95.0000	91.6667
AZ-56	Spoil Pit	0.0596	0.0810	2	37.0000	31.0000
AZ-57	Chal meadow	0.2431	0.2310	1	95.0000	95.0000
AZ-57	Chal meadow	0.2168	0.2030	2	55.0000	93.0000
AZ-58	Chal meadow	0.1806	0.2230	2	49.0000	79.0000
AZ-58	Chal meadow	0.2784	0.2580	1	91.6667	91.6667
AZ-59	Salsoletum nodulosae clayey desert	0.0891	0.0670	1	55.0000	88.3333
AZ-59	Salsoletum nodulosae clayey desert	-0.0107	0.0690	2	5.0000	7.0000

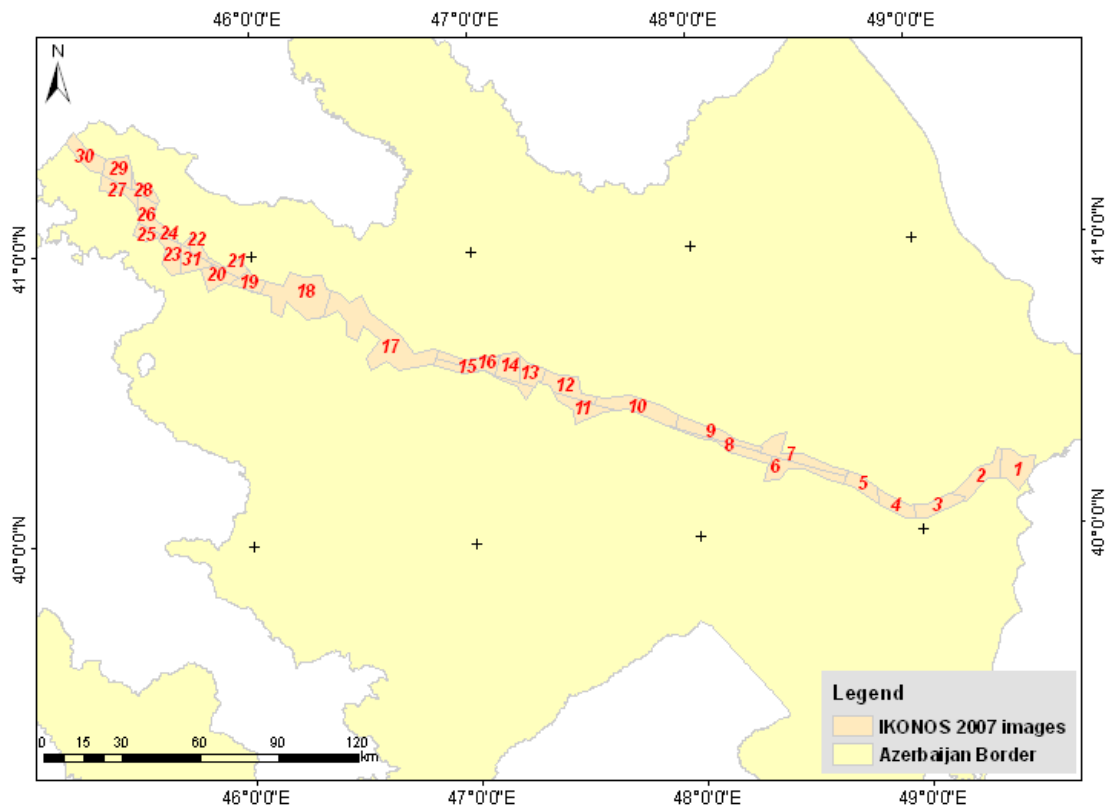
AZ-60	Salsolatum nodulosae clayey desert	0.0917	0.0710	1	95.0000	91.6667
AZ-60	Salsolatum nodulosae clayey desert	-0.0043	0.0650	2	21.0000	7.0000

## APPENDIX 2, Example of Rational Polynomial Coefficients for satellite image

LINE\_OFF: +001080.00 pixels  
 SAMP\_OFF: +002249.00 pixels  
 LAT\_OFF: +40.13210000 degrees  
 LONG\_OFF: +049.39960000 degrees  
 HEIGHT\_OFF: +0064.000 meters  
 LINE\_SCALE: +001080.00 pixels  
 SAMP\_SCALE: +002249.00 pixels  
 LAT\_SCALE: +00.06080000 degrees  
 LONG\_SCALE: +000.11330000 degrees  
 HEIGHT\_SCALE: +0301.000 meters  
 LINE\_NUM\_COEFF\_1: +5.396585600819152E-01  
 LINE\_NUM\_COEFF\_2: +4.098403997124105E-02  
 LINE\_NUM\_COEFF\_3: -1.566415323334366E+00  
 LINE\_NUM\_COEFF\_4: +2.060950837934691E-03  
 LINE\_NUM\_COEFF\_5: -2.445832611917624E-03  
 LINE\_NUM\_COEFF\_6: -1.255476296369393E-03  
 LINE\_NUM\_COEFF\_7: +9.832547693709672E-03  
 LINE\_NUM\_COEFF\_8: -1.369003393477724E-03  
 LINE\_NUM\_COEFF\_9: +1.212024427263089E-02  
 LINE\_NUM\_COEFF\_10: -5.490229709427386E-05  
 LINE\_NUM\_COEFF\_11: +1.050167116016196E-04  
 LINE\_NUM\_COEFF\_12: -1.833222637856031E-06  
 LINE\_NUM\_COEFF\_13: -1.308262601044440E-05  
 LINE\_NUM\_COEFF\_14: +5.541423275251371E-06  
 LINE\_NUM\_COEFF\_15: +8.291429397943759E-06  
 LINE\_NUM\_COEFF\_16: +7.773078584627614E-06  
 LINE\_NUM\_COEFF\_17: +1.075382055060999E-07  
 LINE\_NUM\_COEFF\_18: +1.299257281613031E-05  
 LINE\_NUM\_COEFF\_19: +1.811033470864231E-05  
 LINE\_NUM\_COEFF\_20: +1.208543551287530E-07  
 LINE\_DEN\_COEFF\_1: +1.000000000000000E+00  
 LINE\_DEN\_COEFF\_2: +1.377841978023738E-03  
 LINE\_DEN\_COEFF\_3: -7.764881656388663E-03  
 LINE\_DEN\_COEFF\_4: -6.841280317015611E-03  
 LINE\_DEN\_COEFF\_5: +8.110459315590367E-06  
 LINE\_DEN\_COEFF\_6: -6.038099558873528E-05  
 LINE\_DEN\_COEFF\_7: -5.482560176256859E-06  
 LINE\_DEN\_COEFF\_8: +1.668115231343844E-06  
 LINE\_DEN\_COEFF\_9: -4.940283030420869E-06  
 LINE\_DEN\_COEFF\_10: +3.330197286083899E-06  
 LINE\_DEN\_COEFF\_11: -5.504476052001917E-08  
 LINE\_DEN\_COEFF\_12: -5.006751965783348E-09  
 LINE\_DEN\_COEFF\_13: +3.942526346781926E-09  
 LINE\_DEN\_COEFF\_14: +3.117979674306139E-08

LINE\_DEN\_COEFF\_15: +7.030741331929568E-09  
LINE\_DEN\_COEFF\_16: -4.970131599760191E-09  
LINE\_DEN\_COEFF\_17: -4.661925780693035E-10  
LINE\_DEN\_COEFF\_18: -1.835783527932158E-08  
LINE\_DEN\_COEFF\_19: -1.787348340874009E-08  
LINE\_DEN\_COEFF\_20: -7.478221881056644E-11  
SAMP\_NUM\_COEFF\_1: +1.257216080247078E-02  
SAMP\_NUM\_COEFF\_2: +1.073076335181020E+00  
SAMP\_NUM\_COEFF\_3: +1.341238572440706E-02  
SAMP\_NUM\_COEFF\_4: +2.184072479810670E-02  
SAMP\_NUM\_COEFF\_5: -9.270525153816503E-03  
SAMP\_NUM\_COEFF\_6: -6.604408248604798E-03  
SAMP\_NUM\_COEFF\_7: -2.526702196307066E-04  
SAMP\_NUM\_COEFF\_8: +1.473446523283422E-03  
SAMP\_NUM\_COEFF\_9: -9.639836919392303E-05  
SAMP\_NUM\_COEFF\_10: -1.367712516588300E-04  
SAMP\_NUM\_COEFF\_11: -6.469321759654761E-06  
SAMP\_NUM\_COEFF\_12: +1.902215856843548E-06  
SAMP\_NUM\_COEFF\_13: +1.645582503802057E-06  
SAMP\_NUM\_COEFF\_14: -2.151885641417031E-06  
SAMP\_NUM\_COEFF\_15: +7.513032597704961E-06  
SAMP\_NUM\_COEFF\_16: -1.358196227321960E-07  
SAMP\_NUM\_COEFF\_17: -2.448277388742833E-07  
SAMP\_NUM\_COEFF\_18: -6.364669766483872E-05  
SAMP\_NUM\_COEFF\_19: -6.680603555914807E-07  
SAMP\_NUM\_COEFF\_20: -9.501168567044402E-09  
SAMP\_DEN\_COEFF\_1: +1.000000000000000E+00  
SAMP\_DEN\_COEFF\_2: +1.377841978023738E-03  
SAMP\_DEN\_COEFF\_3: -7.764881656388663E-03  
SAMP\_DEN\_COEFF\_4: -6.841280317015611E-03  
SAMP\_DEN\_COEFF\_5: +8.110459315590367E-06  
SAMP\_DEN\_COEFF\_6: -6.038099558873528E-05  
SAMP\_DEN\_COEFF\_7: -5.482560176256859E-06  
SAMP\_DEN\_COEFF\_8: +1.668115231343844E-06  
SAMP\_DEN\_COEFF\_9: -4.940283030420869E-06  
SAMP\_DEN\_COEFF\_10: +3.330197286083899E-06  
SAMP\_DEN\_COEFF\_11: -5.504476052001917E-08  
SAMP\_DEN\_COEFF\_12: -5.006751965783348E-09  
SAMP\_DEN\_COEFF\_13: +3.942526346781926E-09  
SAMP\_DEN\_COEFF\_14: +3.117979674306139E-08  
SAMP\_DEN\_COEFF\_15: +7.030741331929568E-09  
SAMP\_DEN\_COEFF\_16: -4.970131599760191E-09  
SAMP\_DEN\_COEFF\_17: -4.661925780693035E-10  
SAMP\_DEN\_COEFF\_18: -1.835783527932158E-08  
SAMP\_DEN\_COEFF\_19: -1.787348340874009E-08  
SAMP\_DEN\_COEFF\_20: -7.478221881056644E-11

### APPENDIX 3, Triangulation results for IKONOS and FORMOSAT images



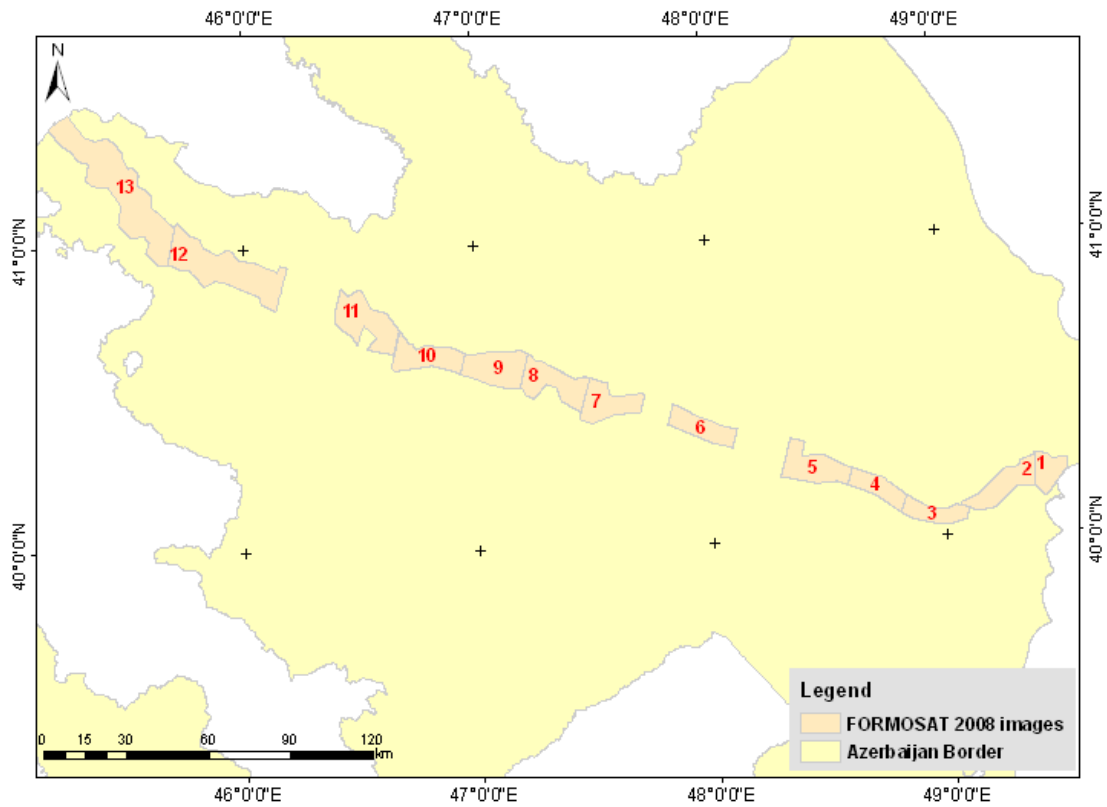
<b>IMAGE NUMBER</b>	<b>1</b>	
<b>RMSE</b>	<b>Pixel</b>	<b>Meter</b>
X	1.130	1.130
Y	0.370	0.370
TOT	1.190	1.190
<b>IMAGE NUMBER</b>	<b>2</b>	
<b>RMSE</b>	<b>Pixel</b>	<b>Meter</b>
X	0.802	0.802
Y	0.572	0.572
TOT	0.985	0.985
<b>IMAGE NUMBER</b>	<b>3</b>	
<b>RMSE</b>	<b>Pixel</b>	<b>Meter</b>
X	0.569	0.569
Y	0.578	0.578
TOT	0.811	0.811
<b>IMAGE NUMBER</b>	<b>4</b>	
<b>RMSE</b>	<b>Pixel</b>	<b>Meter</b>
X	0.440	0.440
Y	0.665	0.665
TOT	0.797	0.797
<b>IMAGE NUMBER</b>	<b>5</b>	
<b>RMSE</b>	<b>Pixel</b>	<b>Meter</b>
X	0.505	0.505
Y	0.410	0.410

TOT	0.650	0.650
<b>IMAGE NUMBER</b>	<b>6</b>	
<b>RMSE</b>	<b>Pixel</b>	<b>Meter</b>
X	0.397	0.397
Y	0.641	0.641
TOT	0.754	0.754
<b>IMAGE NUMBER</b>	<b>7</b>	
<b>RMSE</b>	<b>Pixel</b>	<b>Meter</b>
X	0.820	0.820
Y	1.062	1.062
TOT	1.341	1.341
<b>IMAGE NUMBER</b>	<b>8</b>	
<b>RMSE</b>	<b>Pixel</b>	<b>Meter</b>
X	0.344	0.344
Y	0.411	0.411
TOT	0.536	0.536
<b>IMAGE NUMBER</b>	<b>9</b>	
<b>RMSE</b>	<b>Pixel</b>	<b>Meter</b>
X	0.916	0.916
Y	0.785	0.785
TOT	1.206	1.206
<b>IMAGE NUMBER</b>	<b>10</b>	
<b>RMSE</b>	<b>Pixel</b>	<b>Meter</b>
X	0.875	0.875
Y	0.712	0.712
TOT	1.129	1.129
<b>IMAGE NUMBER</b>	<b>11</b>	
<b>RMSE</b>	<b>Pixel</b>	<b>Meter</b>
X	0.516	0.516
Y	0.885	0.885
TOT	1.025	1.025
<b>IMAGE NUMBER</b>	<b>12</b>	
<b>RMSE</b>	<b>Pixel</b>	<b>Meter</b>
X	0.622	0.622
Y	0.430	0.430
TOT	0.756	0.756
<b>IMAGE NUMBER</b>	<b>13</b>	
<b>RMSE</b>	<b>Pixel</b>	<b>Meter</b>
X	0.406	0.406
Y	1.140	1.140
TOT	1.210	1.210
<b>IMAGE NUMBER</b>	<b>14</b>	
<b>RMSE</b>	<b>Pixel</b>	<b>Meter</b>
X	0.730	0.730
Y	0.928	0.928
TOT	1.181	1.181
<b>IMAGE NUMBER</b>	<b>15</b>	
<b>RMSE</b>	<b>Pixel</b>	<b>Meter</b>
X	0.857	0.857
Y	0.812	0.812
TOT	1.181	1.181
<b>IMAGE NUMBER</b>	<b>16</b>	



<b>RMSE r</b>	<b>Pixel</b>	<b>Meter</b>
X	0.689	0.689
Y	0.867	0.867
TOT	1.107	1.107
<b>IMAGE NUMBER</b>	<b>17</b>	
<b>RMSE</b>	<b>Pixel</b>	<b>Meter</b>
X	0.987	0.987
Y	1.506	1.506
TOT	1.801	1.801
<b>IMAGE NUMBER</b>	<b>18</b>	
<b>RMSE</b>	<b>Pixel</b>	<b>Meter</b>
X	1.204	1.204
Y	0.988	0.988
TOT	1.557	1.557
<b>IMAGE NUMBER</b>	<b>19</b>	
<b>RMSE</b>	<b>Pixel</b>	<b>Meter</b>
X	0.392	0.392
Y	0.615	0.615
TOT (RMSE)	0.729	0.729
<b>IMAGE NUMBER</b>	<b>20</b>	
<b>RMSE</b>	<b>Pixel</b>	<b>Meter</b>
X	0.716	0.716
Y	0.464	0.464
TOT	0.853	0.853
<b>IMAGE NUMBER</b>	<b>21</b>	
<b>RMSE</b>	<b>Pixel</b>	<b>Meter</b>
X	0.688	0.688
Y	0.506	0.506
TOT	0.854	0.854
<b>IMAGE NUMBER</b>	<b>22</b>	
<b>RMSE</b>	<b>Pixel</b>	<b>Meter</b>
X	1.246	1.246
Y	0.713	0.713
TOT	1.436	1.436
<b>IMAGE NUMBER</b>	<b>23</b>	
<b>RMSE</b>	<b>Pixel</b>	<b>Meter</b>
X	0.633	0.633
Y	0.551	0.551
TOT	0.839	0.839
<b>IMAGE NUMBER</b>	<b>24</b>	
<b>RMSE</b>	<b>Pixel</b>	<b>Meter</b>
X	0.525	0.525
Y	0.626	0.626
TOT	0.817	0.817
<b>IMAGE NUMBER</b>	<b>25</b>	
<b>RMSE</b>	<b>Pixel</b>	<b>Meter</b>
X	0.691	0.691
Y	0.821	0.821
TOT	1.073	1.073
<b>IMAGE NUMBER</b>	<b>26</b>	
<b>RMSE</b>	<b>Pixel</b>	<b>Meter</b>
X	0.633	0.633

Y	0.526	0.526
TOT	0.823	0.823
<b>IMAGE NUMBER</b>	<b>27</b>	
<b>RMSE</b>	<b>Pixel</b>	<b>Meter</b>
X	0.314	0.314
Y	0.710	0.710
TOT	0.777	0.777
<b>IMAGE NUMBER</b>	<b>28</b>	
<b>RMSE</b>	<b>Pixel</b>	<b>Meter</b>
X	0.322	0.322
Y	0.478	0.478
TOT	0.577	0.577
<b>IMAGE NUMBER</b>	<b>29</b>	
<b>RMSE</b>	<b>Pixel</b>	<b>Meter</b>
X	0.545	0.545
Y	0.500	0.500
TOT	0.739	0.739
<b>IMAGE NUMBER</b>	<b>30</b>	
<b>RMSE</b>	<b>Pixel</b>	<b>Meter</b>
X	1.291	1.291
Y	1.117	1.117
TOT	1.707	1.707
<b>IMAGE NUMBER</b>	<b>31</b>	
<b>RMSE</b>	<b>Pixel</b>	<b>Meter</b>
X	0.335	0.335
Y	0.608	0.608
TOT	0.694	0.694



<b>IMAGE NUMBER</b>	<b>1</b>	
<b>RMSE</b>	<b>Pixel</b>	<b>Meter</b>
X	1.13	2.26
Y	0.37	0.74
TOT	1.11	2.23
<b>IMAGE NUMBER</b>	<b>2</b>	
<b>RMSE</b>	<b>Pixel</b>	<b>Meter</b>
X	0.81	1.62
Y	1.41	2.81
TOT	1.26	2.52
<b>IMAGE NUMBER</b>	<b>3</b>	
<b>RMSE</b>	<b>Pixel</b>	<b>Meter</b>
X	0.88	1.75
Y	0.88	1.76
TOT	0.96	1.93
<b>IMAGE NUMBER</b>	<b>4</b>	
<b>RMSE</b>	<b>Pixel</b>	<b>Meter</b>
X	0.91	1.83
Y	1.08	2.16
TOT	1.21	2.42
<b>IMAGE NUMBER</b>	<b>5</b>	
<b>RMSE</b>	<b>Pixel</b>	<b>Meter</b>
X	0.47	0.47
Y	0.6	0.6
TOT	0.84	0.84
<b>IMAGE NUMBER</b>	<b>6</b>	
<b>RMSE</b>	<b>Pixel</b>	<b>Meter</b>
X	0.88	1.77

Y	1.14	2.28
TOT	1.23	2.46
<b>IMAGE NUMBER</b>	<b>7</b>	
<b>RMSE</b>	<b>Pixel</b>	<b>Meter</b>
X	0.97	1.93
Y	1.39	2.78
TOT	1.32	2.64
<b>IMAGE NUMBER</b>	<b>8</b>	
<b>RMSE</b>	<b>Pixel</b>	<b>Meter</b>
X	1.45	2.9
Y	0.61	1.21
TOT	1.23	2.47
<b>IMAGE NUMBER</b>	<b>9</b>	
<b>RMSE</b>	<b>Pixel</b>	<b>Meter</b>
X	0.78	1.56
Y	0.8	1.61
TOT	1.09	2.19
<b>IMAGE NUMBER</b>	<b>10</b>	
<b>RMSE</b>	<b>Pixel</b>	<b>Meter</b>
X	0.84	1.68
Y	1.18	2.35
TOT	1.22	2.44
<b>IMAGE NUMBER</b>	<b>12</b>	
<b>RMSE</b>	<b>Pixel</b>	<b>Meter</b>
X	0.53	1.33
Y	0.47	1.17
TOT	1.02	2.56
<b>IMAGE NUMBER</b>	<b>13</b>	
<b>RMSE</b>	<b>Pixel</b>	<b>Meter</b>
X	0.16	0.16
Y	0.9	0.9
TOT	0.84	0.84